

University of Windsor

Scholarship at UWindor

Electronic Theses and Dissertations

Theses, Dissertations, and Major Papers

3-2-2021

Electrospinning of PEO Nanofibers

Nehal Faldu

University of Windsor

Follow this and additional works at: <https://scholar.uwindsor.ca/etd>

Recommended Citation

Faldu, Nehal, "Electrospinning of PEO Nanofibers" (2021). *Electronic Theses and Dissertations*. 8518.
<https://scholar.uwindsor.ca/etd/8518>

This online database contains the full-text of PhD dissertations and Masters' theses of University of Windsor students from 1954 forward. These documents are made available for personal study and research purposes only, in accordance with the Canadian Copyright Act and the Creative Commons license—CC BY-NC-ND (Attribution, Non-Commercial, No Derivative Works). Under this license, works must always be attributed to the copyright holder (original author), cannot be used for any commercial purposes, and may not be altered. Any other use would require the permission of the copyright holder. Students may inquire about withdrawing their dissertation and/or thesis from this database. For additional inquiries, please contact the repository administrator via email (scholarship@uwindsor.ca) or by telephone at 519-253-3000ext. 3208.

Electrospinning of PEO Nanofibers

By

Nehal Faldu

A Thesis

Submitted to the Faculty of Graduate Studies
through the Department of Mechanical, Automotive and Materials Engineering
in Partial Fulfillment of the Requirements for
the Degree of Master of Applied Science
at the University of Windsor

Windsor, Ontario, Canada

2020

© 2020 Nehal Faldu

Electrospinning of PEO Nanofibers

By

Nehal Faldu

APPROVED BY:

O. Jianu

Department of Mechanical, Automotive and Materials Engineering

H. Hu

Department of Mechanical, Automotive and Materials Engineering

D. Northwood, Co-Advisor

Department of Mechanical, Automotive and Materials Engineering

R. Riahi, Co-Advisor

Department of Mechanical, Automotive and Materials Engineering

November 25, 2020

DECLARATION OF CO-AUTHORSHIP

I hereby declare that this thesis incorporates material that is the result of joint research, as follows:

In all cases, the key ideas, primary contributions, experimental designs, data analysis, and interpretation were performed by the author Nehal Faldu, Dr. Derek Northwood as an advisor and Dr. Reza Riahi as co-advisor. Chapter 4 contains selected results from the collaborative research with Iman A. Borojeni. These results can be found in: Tables 4.2, 4.3, and 4.4; Figure 4.2 A & B; Figure 4.4; part of Figure 4.10 (a); selected results in Figure 4.11 and Figure 4.12. I certify that, with the above qualification, this dissertation and the research it refers to are the product of my work.

I am aware of the University of Windsor Senate Policy on Authorship, and I certify that I have properly acknowledged the contribution of other researchers to my thesis and have obtained written permission from each of the co-author(s) to include the above material(s) in my thesis.

I certify that, with the above qualification, this thesis, and the research to which it refers, is the product of my work.

I declare that, to the best of my knowledge, my thesis does not infringe upon anyone's copyright nor violate any proprietary rights and that any ideas, techniques, quotations, or any other material from the work of other people included in my thesis, published or otherwise, are fully acknowledged in accordance with the standard referencing practices. Furthermore, to the extent that I have included copyrighted material that surpasses the bounds of fair dealing within the meaning of the Canada Copyright Act, I certify that I have obtained written permission from the copyright owner(s) to include such material(s) in my thesis.

I declare that this is a true copy of my thesis, including any final revisions, as approved by my thesis committee and the Graduate Studies office and that this thesis has not been submitted for a higher degree to any other University or Institution.

ABSTRACT

Electrospinning is a method centered on electrostatic forces for fabricating continuous nanofibers with a substantial active surface area per mass unit. One of the essential parameters that affect a polymer's ability to create nanofibers is the chain length, given by the molecular weight. In this study, polyethylene oxide (PEO) with molecular weights from 100,000 to 5,000,000 g/mol were used to investigate the effect of molecular weight on the shape, size, and morphology of the fabricated fibers. The electrospinning experiments were conducted at flow rates ranging from 4.16 to 16.67 $\mu\text{L}/\text{min}$ and working distances between 10 and 20 cm. The collected fibers were analyzed using Scanning Electron Microscopy (SEM). Based on the solution and processing conditions, different structures from droplets, and heavily beaded fibers to defect-free mats were obtained. PEO's water-based solutions produced bead free fibers for molecular weights in the range of 100,000 to 900,000 g/mol for a range of processing conditions. However, the processing window for the formation of bead free fibers was more restricted for water-ethanol solutions than for deionized water solutions. Furthermore, the electrospun jet of ultra-high molecular weight PEO (5,000,000 g/mol) solutions showed very small bending instabilities, which reduced the chance of drying the jet during its flight time, even with a relatively high working distance (20cm). Therefore, the products exhibited over-wetting and film formation. The results are discussed in terms of the viscosity and entanglement number, $(n_e)_{\text{soln}}$, of the PEO solution.

DEDICATION

To Thakorji, I can do all things through him who gives me strength.

To my parents, Mr. Umesh Faldu and Mrs. Nita Faldu, who showed me how to love, taught me the importance of education, always encouraged me to pursue my dreams, and supported me in immeasurable ways throughout it all.

To my younger brother Rushi Faldu, my best friend, your strength and dedication over the past few years is a daily motivation to work hard and be thankful for the many blessings I have been given.

To my grandfather, Dr. Devshi Makhansa, you are a lifelong teacher. To my grandmother, Mrs. Saita Makhansa, your life experiences are what led me to become a better human being.

ACKNOWLEDGEMENTS

I would first like to thank my thesis advisor Dr. Derek Northwood at the University of Windsor. Dr. Derek Northwood's office's door was always open whenever I ran into a trouble spot or had a question about my research or writing. He consistently allowed this thesis to be my work but steered me in the right direction whenever he thought I needed it.

I would also like to thank my thesis co-advisor Dr. Reza Riahi who designed and built the electrospinning equipment for this research project. I wish to show my appreciation for providing me with the equipped lab and your kind support throughout my research.

I want to thank the following people for helping me finalize the project. Thanks to Dean Mehrdad Saif, Dean Patricia Weir, Dr. Scott Goodwin, and Dr. Daniel Green, Angela Haskell, Denise Lauzon, Amal Jammali, and Deena Wang.

I would like to recognize the invaluable assistance that Dr. Afsaneh Edrisy and all my lab members have provided during my study. Thanks to Iman A. Borojeni, Dr. Olufisayo Gali, Razieh Kiani Harchegani, Javad Mohammadi, Lucas Chauvin, Joselyne Mcphedran, Junhui Ma.

Thank you to my committee members Dr. Ofelia Jianu and Dr. Henry Hu, for taking the time to review my thesis and provide feedback throughout my research.

I am very grateful to Mr. Andy Jenner, Mr. Steve Budinsky, and Ms. Sharon Lackie for their technical assistance in the experimental analysis, tests, informative and valuable discussion in this research.

Lastly, I would like to thank my parents Umesh Faldu and Nita Faldu, brother Rushi, Jayesh Vachhani Uncle, my and some of my close people Tapan Patel, Bart Hoxha, Deepali Jha, Rudresh Jha, Saloni Sancheti, Sheetal Rathod, Bharanidharan Rajasekaran, and Saarah Akhand for providing me with unfailing support and continuous encouragement throughout my years of study and through the process of researching and writing this thesis. Without you all, I would not be where I am today, and I am genuinely appreciative of all the support you have provided me along the way.

TABLE OF CONTENTS

DECLARATION OF CO-AUTHORSHIP	iii
ABSTRACT	iv
ACKNOWLEDGEMENTS.....	vi
LIST OF TABLES	ix
LIST OF FIGURES	x
LIST OF ABBREVIATIONS/SYMBOLS	xiii
CHAPTER 1 INTRODUCTION	1
1.1 Motivation.....	1
1.2 Scope of Research	3
1.3 References.....	6
CHAPTER 2 LITERATURE REVIEW	9
2.1 Nanofibers and their application.....	9
2.2 Methods of the production of polymeric nanofibers	10
i. Drawing.....	10
ii. Template Synthesis.....	11
iii. Phase Separation	12
iv. Self-Assembly.....	13
v. Electrospinning	14
2.3 Comparison of methods for the production of nanofibers.....	15
2.4 Electrospinning: Working principles and equipment setup	16
2.5 Parameters controlling electrospun product form	19
2.5.1 Processing parameters.....	19
2.5.2 Materials Parameters.....	21
2.5.3 Environmental Parameters	23
2.6 Polyethylene Oxide (PEO).....	24
2.7 Electrospinning of PEO.....	26
2.8 References	29

CHAPTER 3 EXPERIMENTAL DETAILS	40
3.1 Design and Construction of Purpose-built Electrospinning Equipment	40
3.2 Experimental Details for the Exploratory Study	42
3.2.1 Materials (PEO and Solvents) used	42
3.2.2 Preparation of Solutions for Electrospinning.....	43
3.2.3 Operating Procedures for Electrospinning.....	43
3.2.4 Preparation and Characterization of Electrospun Product.....	44
3.3 References.....	46
CHAPTER 4 RESULTS AND DISCUSSION	47
4.1 Summary of Results.....	47
4.2 Morphology of Electrospun Nanofibers.....	52
4.3 Effect of Molecular Weight & Solution Concentration on the morphology of nanofibers	54
4.4 Effect of Solvent on the morphology of nanofibers.....	58
4.5 Effect of Voltage on the morphology of nanofibers	59
4.6 Effect of Distance from needle tip to the collector on the morphology of nanofibers	60
4.7 Effect of Flow Rate on the morphology of nanofibers.....	61
4.8 Image J analysis of fiber diameter	63
4.9 Effect of Viscosity/Intrinsic Viscosity on the morphology of nanofibers.....	65
4.10 Effect of Entanglement Number on morphologies of nanofibers.....	68
4.11 References	72
CHAPTER 5 CONCLUSIONS AND SUGGESTIONS FOR FUTURE WORK...76	
5.1 Conclusions.....	76
5.1.1 Electrospinning equipment.....	76
5.1.2 Exploratory study	76
5.2 Suggestions for future work.....	79
5.3 References	80
VITA AUCTORIS.....	82

LIST OF TABLES

Table 2. 1 (a) Comparison of processing techniques for obtaining nanofibers	16
Table 2. 1 (b) Advantages and disadvantages of various processing techniques	16
Table 3. 1 Various molecular weight of PEO	42
Table 3. 2 Solvents used in the study	43
Table 3. 3 Step-by-step procedures for electrospinning.....	44
Table 4. 1 presents the data for PEO with a molecular weight of 100,000 g/mol	48
Table 4. 2 presents the data for PEO with a molecular weight of 600,000 g/mol	49
Table 4. 3 presents the data for PEO with a molecular weight of 900,000 g/mol	50
Table 4. 4 presents the data for PEO with a molecular weight of 5,000,000 g/mol	51
Table 4. 5 The effect of collector distance and flow rate on the average, maximum, and minimum diameters (\pm standard deviation from Image J software)	64
Table 4. 6 Viscosity of solutions of PEO of varying molecular weight in water (all 5% solutions unless otherwise indicated).....	65
Table 4. 7 Intrinsic viscosity of PEO in water [24].....	666
Table 4. 8 Effect of Molecular weight, Concentration, and Solvent on the electrospun product for PEO	67

LIST OF FIGURES

Figure 1.1 Applications of Nanofibers.....	2
Figure 1.2 Stages of research	4
Figure 1.3 Brief descriptions of the design of electrospinning equipment	4
Figure 1.4 Range of products.....	5
Figure 1.5 Materials and Processing parameters investigated	6
Figure 2.1 Obtaining nanofibers by drawing [15].....	11
Figure 2.2 Obtaining nanofibers by template synthesis [18]	12
Figure 2.3 Obtaining nanofibers by phase separation synthesis [22]	13
Figure 2.4 Obtaining nanofiber by self-assembly [23]	14
Figure 2.5 A basic electrospinning device [25]	18
Figure 2.6 Materials and Processing Parameters	19
Figure 2.7 Schematic representation of PEO clustering in water due to end chain effect [72].....	26
Figure 3.1 The purpose-built setup for electrospinning instrument in the lab: (a)Needle (b)movement controller (c)solution tube (d)cylinder shaped sample collector (e)syringe driver pump (f)high voltage DC power supply (g)humidity controller (h)temperature control	41
Figure 3.2 FEI Quanta 200 FEG Environmental SEM	45
Figure 3.3 Nanofiber sample preparation for SEM.....	46
Figure 4.1 Range of products.....	53

Figure 4.2 The SEM micrographs of the electrospun fibers from the different molecular weights of PEO water solution when flow rate (F) = 6 μ L/min and working distance (D) = 20 cm.....	55
Figure 4.3 The SEM micrographs (SE) of the electrospun deposition (beaded fibers, fibers, and film) from different concentrations(C) of PEO (900 KDa) in water-ethanol solution when the flow rate = 6 μ L/min and working distance = 20cm	56
Figure 4.4 Variation in morphology of electrospun nanofibers of PEO with viscosity: (a–d) [12].....	57
Figure 4.5 The SEM micrographs of the electrospun fibers from 100 KDa PEO with concentration 18 % under different solvents and constant voltage (kV), working distance (D), flow rate (F).....	58
Figure 4.6 The SEM micrographs of the electrospun fibers from 100 KDa PEO water-ethanol solution with concentration 18 % under different voltages (kV), constant working distance (D) and flow rate (F).....	60
Figure 4.7 The SEM micrographs of the electrospun fibers from 100 KDa PEO water-ethanol solution with concentration 30 % under different working distances (D) and constant flow rates (F)	61
Figure 4.8 The SEM micrographs of the electrospun fibers from 100 KDa PEO water solution with concentration 30 % under different flow rates (F) and a constant working distance (D).....	62
Figure 4.9 Entanglements in polymer melts [26].....	68
Figure 4.10 (a) The relationship between the entanglement number ((ne) soln) and the morphology of the electrospun product	70

Figure 4.10 (b) SEM color-coded micrographs to correspond to a particular morphology of the produced by electrospinning	70
Figure 4.11 Graphic representation of solution concentration (%) vs entanglement number ((ne) soln) of different molecular weight of PEO in water solution	71
Figure 4.12 Graphic representation of solution concentration (%) vs entanglement number ((ne) soln) of different molecular weight of PEO in water-ethanol solution	72
Figure 5.1 Summary of materials and processing parameters investigated in the exploratory study	77
Figure 5.2 Electrospinning setup consisting of a high-voltage power supply, a syringe, a syringe pump, and a nanofiber collector (illustrated as seen from the edge of a black flat plate) [3]	80

LIST OF ABBREVIATIONS/SYMBOLS

- PEO** - Poly (ethylene oxide)
- DC**- Direct Current
- AC**- Alternating Current
- DMF**- Dimethylformamide
- PEG** - Poly (ethylene glycol)
- FDA** – Food and Drug Administration
- SPE** - Solid polymer electrolytes
- PDI**- Polydispersity Index
- PVA** – Poly (vinyl alcohol)
- PVDF**- Polyvinylidene Fluoride
- OM**- Optical Microscopy
- SEM**- Scanning Electron Microscopy
- ESEM**- Environmental Scanning Electron Microscopy
- DNA** - Deoxyribonucleic acid
- EDAX** - Energy Dispersive X-Ray Analysis
- EDS** - Energy-dispersive X-ray spectroscopy
- SDD** - Silicon Drift **D**etector (**SDD**)
- FEG** - Field Emission Gun
- DoE**- Design of Experiment
- AFD**- Average Fiber Diameter
- wt% - weight percent
- mL - milliliter
- cm - centimeter
- nm - nanometer

kDa - kilodalton
n - degree of polymerization
Å - Angstrom
NaCl – Sodium chloride
Ce - Entanglement Concentration
Mw – Molecular weight
Mn - mass average molecular weight
qv- volume charge density
kV- Kilovolts
ms⁻¹ - meter per second
SiO₂ - Silicon dioxide
CaO – Calcium oxide
Rpm – Revolutions per minute
ml/g – Milliliter per gram
η - Intrinsic viscosity
mPa.s - millipascal-seconds
P - Poise
cP - Centipoise
g/mol – gram per mol
μL/min – Microliter per minute
η_e - entanglement number

CHAPTER 1

INTRODUCTION

This research is based on the production of nanofibers of PEO (Polyethylene Oxide) using an electrospinning technique. The research can be divided into two phases:

1. Design and construction of purpose-built electrospinning equipment.
2. Exploratory study to examine the effect of material and processing parameters on producing nanofibers of PEO.

1.1 Motivation

(i) Nanofibers:

The term nanofiber can be divided into two sections, namely "nano" and "fiber". The textile business describes fibers as a thread, natural or synthetic, e.g., cotton or nylon, spun into a yarn. A "fiber" is defined from a geometrical perspective as a lean, elongated, threadlike object or structure [1]. The term "nano" is defined as a billionth of the unit. Usually, the nanofiber is a term used for fibers with a thickness of less than 100 nanometers [2]. Nanofibers are much smaller than a strand of a human hair (5-150 microns) or a pollen grain (20-30 microns) [3].

They are challenging to see with the naked eye, so they are examined utilizing magnification. Substantive studies have been made on spider dragline silks and show that a spider dragline's strength is significantly tougher than a steel fiber of the identical size [4]. The diameters of nanofibers depend on both the type of polymer and its process of fabrication. Nanofibers can be produced from a broad range of polymers. Nanofibers can be utilized in small, cost-effective blood purification techniques to substitute for dialysis [5]. Nanofibers are utilized to encapsulate specific cancer cells flowing in the bloodstream. They utilize nanofibers covered with antibodies that attach to cancer cells, catching the cancer cell for assessment. Nanofibers can also promote the creation of cartilage in injured joints [6].

Nanofibers show extraordinary properties, basically due to the outstandingly high surface to weight ratio compared to old-fashioned nonwovens. The large surface area accessible on a

nanofiber makes it especially useful for innovations that require large surface areas for chemical reactions to happen. Increasing the surface area speeds up a chemical reaction. Low density, high porosity- good breathability, high pore volume [7], and tight pore size make the nonwoven nanofiber suitable for a broad array of filtration uses.

Nanofibers are an exciting new range of materials that are being utilized in a wide range of applications: see Figure 1.1

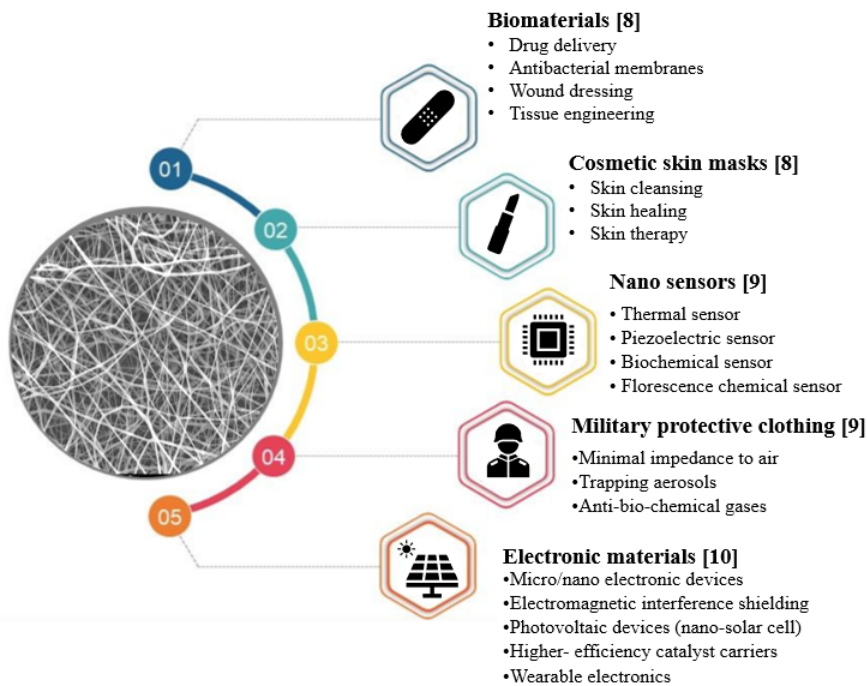


Figure 1.1 Applications of Nanofibers

(ii) Production of Nanofibers:

There are several techniques capable of fabricating nanofibers. These techniques include drawing, template synthesis, phase separation, self-assembly, and electrospinning [11]. For this research, the electrospinning technique was selected to produce fine nanofibers.

Electrospinning is one of the most widely recognized strategies for delivering polymer nanofibers. The conventional setup allows a polymer solution to pass through a needle while being exposed to a high voltage electric field. The electric field's high electric force generates a

Taylor cone at the tip of the needle, from which fibers are then stretched to the collector of the electrospinning device [12]. The product and the quality of the nanofibers are determined by the type of polymer; solvent; concentration of polymer, applied voltage; distance from the solution ejector (needle) to the collector; electrostatic field strength. Each polymer, combined with an appropriate solvent, has a specific range of processing parameters to form nanofibers [13]. The voltage and distance are interchangeable since a higher voltage provides the flexibility for the larger ejector to collector distances, and vice versa [12]. To produce high-quality fibers, the distance between the ejector and the collector must be sufficient for the solvent to evaporate entirely before reaching the collector. It should likewise not evaporate excessively fast, which leaves a solidified polymer that obstructs the spinning process.

(iii) Why PEO?

Poly (ethylene glycol) (PEG), also called poly (oxyethylene) or poly (ethylene oxide) (PEO), is an engineered polyether that is readily accessible in a range of molecular weights. Materials with $M_w < 100,000$ are generally called PEGs, whereas higher molecular weight polymers are classified as PEOs [14]. These polymers are amphiphilic and dissolvable in water and various organic solvents (e.g., methylene chloride, ethanol, toluene, acetone, and chloroform). Low molecular weight ($M_w < 1,000$) PEGs are viscous and colorless liquids, whereas higher molecular weight PEGs are waxy, white solids with melting points that are proportionate to their molecular weight [15]. PEG is nontoxic and is authorized by the FDA for use as a carrier in various pharmaceutical inventions, foods, and beauty care products [16]. Due to their higher molecular weight, PEOs are appropriate for hydrogel arrangement or formation of small molecules. PEO is a highly crystalline polymer, biocompatible, porous material, and biodegradable [17]. Solid polymer electrolytes (SPEs) are among the most promising approaches to the fabrication of safe and lightweight lithium secondary batteries [18]. PEO, in the form of a nanofibrous membrane, is showing considerable promise as an SPE [19].

1.2 Scope of Research

The stages of the research are summarized in Figure 1.2



Figure 1.2 Stages of research

The intent of this research was to build custom designed electrospinning equipment and study the effects of materials and processing parameters on the product. As such, it was both a platform for scientific research and could also function as a laboratory nanofiber production unit for potential upgrading to industrial production. Furthermore, the equipment should be compatible with adjustable components. The equipment should be user-friendly, cost-effective, and small enough to fit on a conventional counter in the laboratory. The components must be resistant to any solvent used in the spinning procedure. The equipment should include as few custom parts as possible to maintain costs at a low level and simplify the construction process of the equipment. When considering the design of the electrospinning equipment, attention was focused on whether to use a single or complex needle, a horizontal or vertical setup, and a stationary or rotating collector. These considerations are summarised in Figure 1.3

Why single Needle?	Why rotating collector?
<ul style="list-style-type: none"> • Controlled flow-rate • Bead formation can be minimised • Fiber morphology and quality are precisely controlled • Allows for a wide variety of materials including high volatile solvents • Minimising solution waste • Laboratory scaled electrospinning 	<ul style="list-style-type: none"> • It allows to produce nanofibers in a large area • Unique structure • Fiber diameter and uniformity varies depending on the type of collectors • Electric field at the central part of cylinder spinneret is much lower than the electric field at the edges
Why horizontal type setup?	
<ul style="list-style-type: none"> • Gravity is the main difference • Direction of gravity and electric field forced on fibers are perpendicular 	

Figure 1.3 Brief descriptions of the design of electrospinning equipment

In the initial exploratory study of the effects of material and processing parameters on the product, the product form varied from beaded nanofibers to a film: see Figure 1.4. Our aim was to produce defect-free fine nanofibers through electrospinning. During the process of producing fine nanofibers, many different structures were explored. Each type of product has its application.

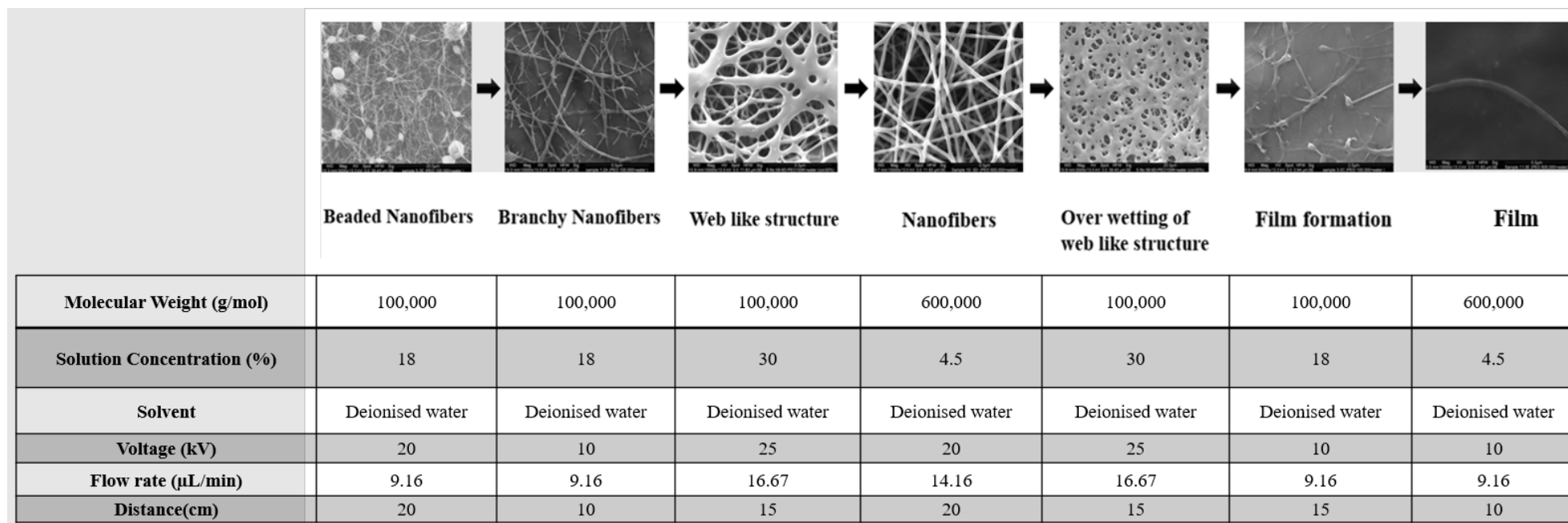


Figure 1. 4 Range of products

The limited number of material and process parameters that were examined is illustrated in Figure 1.5. The focus of this research was "Materials Parameter" Molecular Weight of PEO, which ranged from 100,000 to 5,000,000 g/mol.

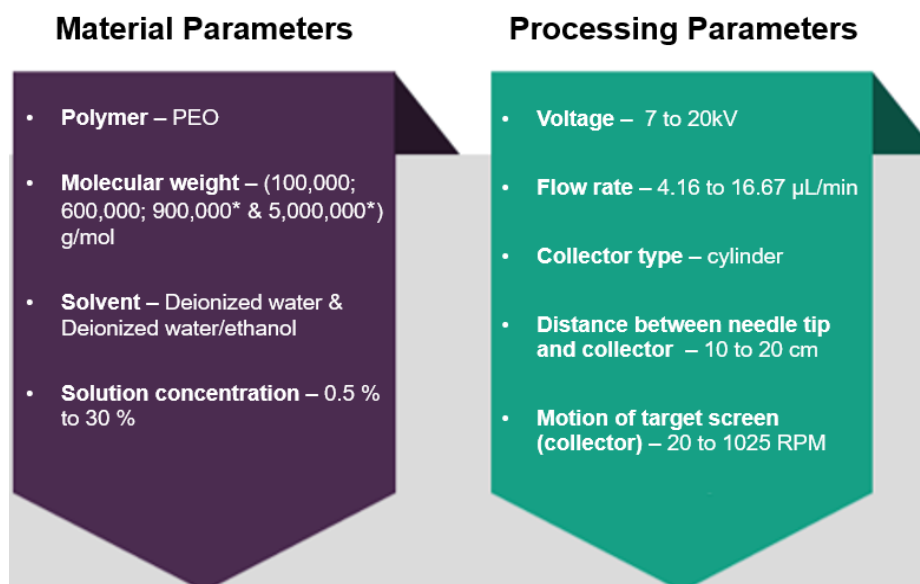


Figure 1. 5 Materials and Processing parameters investigated

All electrospun products were characterized for both form and dimensions using optical microscopy (OM), scanning electron microscopy (SEM), and Image J software. The results of this study are analyzed in terms of a polymer-solvent parameter known as the entanglement number, which is related to the molecular weight and concentration of PEO [20-22].

1.3 References

- 1) Ramakrishna, S., Fujihara, K., Teo, W.E., Lim, T.C., and Ma, Z. An introduction to electrospinning and nanofibers. World Scientific Publishing Co. Pte. Ltd, USA, (2015).
- 2) Ko, F. K., and Wan, Y. Introduction to Nanofiber Materials. Cambridge University Press, United Kingdom, (2014).
- 3) Malayeri, B., Noori, M., and Jafari, M. Using the pollen viability and morphology for fluoride pollution biomonitoring. Biological Trace Element Research, Vol. 147, No. 1-3, pp.315-319 (2011).
- 4) Kaplan, D., Adams, WW., Farmer, B., and Viney, C. Silk polymers: material science and biotechnology. 1st ed. Washington, DC: ACS Symposium Series 1993.

- 5) Dersch, R., Steinhart, M., Boudriot, U., Greiner, A., and Wendorff, J.H. "Nano processing of polymers: applications in medicine, sensors, catalysis, photonics," *Polymers for Advanced Technologies*, Vol. 16, No. 2-3, pp. 276–282 (2005).
- 6) Fang, J., Wang, X., and Lin, T. "Functional applications of electrospun nanofibers," in *Nanofibers-Production, Properties and Functional Applications*, pp. 287–326, Intech, 2011.
- 7) Martins, A., Araujo, J. V., Reis, R. L., and Neves, N. M. "Electrospun nanostructured scaffolds for tissue engineering applications," *Nanomedicine*, Vol. 2, No. 6, pp. 929–942 (2007).
- 8) Zhang, L., Chae, S.R., Hendren, Z., Park, J.S., and Wiesner, M. R. "Recent advances in proton exchange membranes for fuel cell applications," *Chemical Engineering Journal*, Vol. 204-205, pp. 87–97 (2012).
- 9) Kumar, G. G., and Nahm, K. S. "Polymer nanocomposites fuel cell applications," in *Advances in Nanocomposite-Synthesis, Characterization and Industrial Applications*, pp. 639–660, Intech Europe, Vienna, Austria, 2011.
- 10) Luzio, A., Canesi, E.V., Bertarelli, C., and Caironi, M. Electrospun polymer fibers for electronic applications, *Materials*, Vol. 7, pp. 906-947 (2014).
- 11) Baji, A., Mai, Y.W., Wong, S.C., Abtahi, M., and Chen, P. "Electrospinning of polymer nanofibers: effects on oriented morphology, structures, and tensile properties," *Composites Science and Technology*, Vol. 70, No. 5, pp. 703–718 (2010).
- 12) Li D., and Xia Y. Electrospinning of nanofibers: reinventing the wheel? *Advanced Materials*, Vol. 16, pp. 1151–1170 (2004).
- 13) Greiner A., and Wendorff JH. Electrospinning: a fascinating method for the preparation of ultrathin fibers. *Angewandte Chemie Int Ed*, Vol. 46, pp. 5670–703 (2007).

- 14) Dimitrov, I., and Tsvetanov, C. B. in *Polymer Science: A Comprehensive Reference*; Vol. 4, pp 551–569; Penczek, S.; Grubbs, R. H., Eds.; Matyjaszewski, K., Möller, M. Series Eds.; Elsevier: Amsterdam, 2012.
- 15) Klein, R., and Wurm, F. R. *Aliphatic Polyethers: Classical Polymers for the 21st Century. Macromolecular Rapid Communications*, Vol. 36, pp. 1147–1165 (2015).
- 16) Fruijtier-Pölloth, C. *Safety Assessment on Polyethylene Glycols (PEGs) and Their Derivatives as Used in Cosmetic Products. Toxicology*, Vol. 214, pp. 1-38 (2005).
- 17) Ma, P.X. *Tissue engineering. In Kroschwitz, JI editor. Encyclopedia of Polymer Science and Technology 3rd Edition. John Wiley & Sons (New Jersey). pp. 261-291 (2004).*
- 18) Verma, P., Maire, P., and Novák, P. *A Review of the Features and Analyses of the Solid Electrolyte Interphase in Li-ion Batteries. Electrochimica Acta.*, Vol. 45, pp. 6332-6341 (2010).
- 19) Banitaba, S.N., Semnani, D., Fakhrali, A., Ebadi, SV., Heydari-Soureshjani, E., Rezaei, B., and Ensafi, AA. *Electrospun PEO nanofibrous membrane enables by LiCl, LiClO₄, and LiTFSI salts: a versatile solvent-free electrolyte for lithium-ion battery application. Ionics*, Vol. 26, pp. 3249-3260 (2020).
- 20) MacDiarmid, A. G., Jones Jr, W. E., Norris, I. D., Gao, J., Johnson Jr, A. T., Pinto, N. J., Hone, J., Han, B., Ko, F. K., Okuzaki, H., and Llaguno, M. *Electrostatically-generated nanofibers of electronic polymers. Synthetic Metals*, Vol. 119, pp. 37–40 (2001).
- 21) Wool, R.P. *Polymer entanglements. Macromolecules*, Vol. 26, No. 7, pp. 1564-1569 (1993).
- 22) Shenoy, S.L., Bates, W.D., Frisch, H.L., and Wnek, G.E. *Role of chain entanglements on fiber formation during electrospinning of polymer solutions: good solvent, non-specific polymer-polymer interaction limit. Polymer*, Vol. 46, pp. 3372-3384 (2005).

CHAPTER 2

LITERATURE REVIEW

2.1 Nanofibers and their application

Nanofibers have diameters on the nanometer scale. The nanofibers are well-defined as a nano object with two comparable outer dimensions in the nanoscale (0–100 nm) and the third dimension significantly greater. Nanofibers have drawn significant attention in recent times. They have exciting size-dependent biological, chemical, electrical, thermal, mechanical, optical, and magnetic properties because of their one-dimensionality [1]. The exceptional optical and electrical properties are discovered as compared to other dimensionalities. Nanofiber production is a demanding and essential research topic because of their unique size- and shape-dependent properties. Presently, several researchers have been successfully fabricating nanofibers from inorganic and organic precursors. Nanofibers can be utilized in several conventional applications and surround us in routine life, including batteries, fuel cells, solar cells, mobiles, and ultra-filtration membranes [2-4]. The fiber diameter determines the specific surface area. The fiber morphology provides immense flexibility in tuning the properties of nanofibers [5].

Various nanofiber materials, including metal, metal oxides, carbon, and polymers, can be utilized to produce nanofibers. Different physicochemical factors like length, diameter, inter-fiber spacing, Young's Modulus, and adhesion energy are considered in designing nanofibers [6]. Surface modified nanofibers with chemical compounds and nanomaterials have attracted lots of interest in new applications as well. These surface modified nanofibers with functional groups showed better removal property of nanofiber absorbent for heavy metal ions, many organic dyes either by electrostatic interaction or chelation [7].

Nanofibers, due to their very high surface to volume ratio compared with traditional strands, show exciting properties, for instance, low thickness, low specific mass, and high pore volume, which make them a good fit for a broad scope of uses, for instance, filtration and energy storage [8,9]. Nanofibrous mats with specific pore sizes are utilized as chemical and mechanical filters. These are preferably appropriate for filtering submicron particles from air or water. The effectively created fibrous mat can trap and dissolve the chemical and biological elements through chemical effects. These strands joined with other nonwoven items, have potential uses in

a broad array of filtration applications, such as aerosol filters, facemasks, defensive clothing, personal care items, wipes, clothing, and insulation [2,3]. Textiles made with microfibers guarantee stain resistance and a very fine texture. Currently, military fabrics, a work in progress intended for chemical and biological protection, have been improved by including a layer of nanofibers between the bodyside layer and the carbon fibers [10]. Nanofibers are likewise applied in clinical applications, which incorporate medication and gene delivery, artificial blood vessels, artificial organs, tissue engineering, and medical facemasks [11]. For instance, carbon fiber hollow nanotubes, tinier than blood cells, can convey drugs into blood cells. Different nanofibers are in aviation capacitors, semiconductors, battery separators, energy storage, fuel cells, and data innovation [2-4].

Nanofibers of conducting polymers are forecast to have exceptional electronic and optical properties that can be tuned through doping. These sorts of fibers have the potential for a wide range of uses in chemical and biological sensors, light-emitting diodes, rechargeable batteries, nano-electronic gadgets, electromagnetic protecting, and wearable electronics. Likewise, nanofibers obtained from ceramic materials, such as zinc oxide and silicon carbide, have optical qualities (glow) that can be utilized in light and field emitters [12]. The fibers are additionally utilized widely as a back-up in the improvement of nanocomposites.

2.2 Methods of the production of polymeric nanofibers

Several techniques, like Drawing, Template Synthesis, Phase Separation, Self-Assembly, and Electrospinning, have been used to synthesize the polymeric nanofibers.

i. Drawing

In the drawing method, the single nanofiber is formed by extending a polymer that is in the form of a solution. A standard drawing process needs a SiO₂ surface, a micropipette, and a micromanipulator to create nanofibers. A micropipette, some micrometers in diameter, is dipped into the droplet close to the contact line through a micromanipulator. The micropipette is then taken out from the alcohol at a speed of around $1 \times 10^{-4} \text{ ms}^{-1}$ to pull a nanofiber. The pulled fiber is deposited on a surface by contacting it with the micropipette end. The nanofiber drawing is repeated on every droplet. The material consistency at the edge of the droplet increased with evaporation. The procedure must be applied to viscoelastic materials that can tolerate a high degree of deformation while remaining strong enough to hold up the created stress during pulling

[13]. If the polymer is in a molten state, at that point, the cooling framework is vital to set the fiber.

Moreover, if the polymer is in a solution state, at that point, a warming system is essential to volatilize the solvent. It is a delayed cycle that is appropriate for lab-scale, which keeps it from being scaled up to an industrial level [14]. Figure 2.1 is a schematic diagram showing nanofiber production by drawing [15].

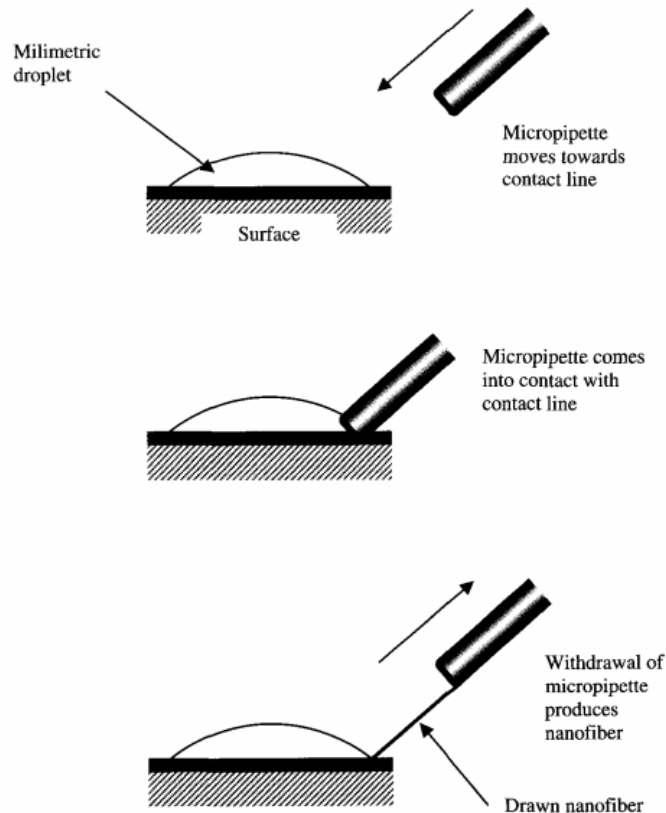


Figure 2. 1 Obtaining nanofibers by drawing [15]

ii. Template Synthesis

Template synthesis involves the utilization of a template or mold to acquire an ideal material or structure. The casting method and DNA replication can be considered as template-based synthesis [16]. In the case of nanofiber creation, the template refers to a metal oxide membrane with through-thickness pores of nanoscale diameter [17]. The use of water pressure on one side, and control from the porous membrane, causes extrusion of the polymer, which, after

encountering a solidifying solution, gives rise to nanofibers whose diameters are determined by the pores. In this procedure, porous membranes are utilized in which pores are cylinder-shaped. The diameters of these pores are uniform. Solid polymers are created that have a diameter equivalent to the size of the pores. Figure 2.2 is a schematic of template synthesis [18]. Template synthesis is a comparatively easy, and economical method to generate fibers.

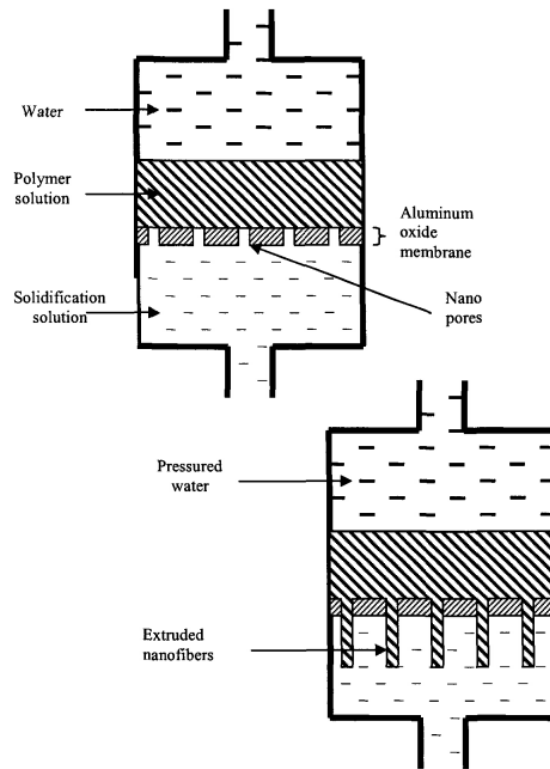


Figure 2. 2 Obtaining nanofibers by template synthesis [18]

iii. Phase Separation

During this process, five steps are involved: polymer dissolution, polymer gelation, solvent extraction, freezing, and freeze-drying. Fiber dimensions do not seem to be manageable with this process. This approach is only appropriate for laboratory scale [19]. In phase separation, a polymer is blended with a solvent before undergoing gelation. The primary mechanism in this procedure is the separation of phases owing to physical change. The solvent phase is then removed, leaving behind the additional residual phase. The phase separation procedure has been studied and investigated to produce microporous membranes for different tissue engineering and electronics applications. In this technique, polymer gelation takes place, and the gel extracts the

solvent. Typically, water is used to replace the solvent in the gel. The gel is freeze-dried under a vacuum to remove the water. The membrane's porous morphology can be controlled during the gelation process by adjusting the polymer concentration, type of polymer, type of solvent, and temperature [20]. Also, the incorporation of paraffin spheres, salt, and sugar, has been examined to control the membrane [21]. Figure 2.3 is a schematic for phase separation synthesis [22].

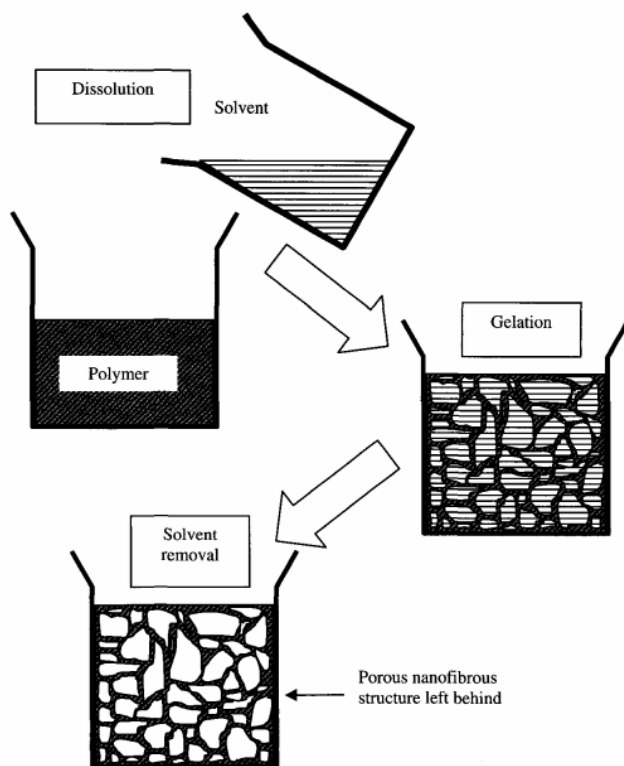


Figure 2. 3 Obtaining nanofibers by phase separation synthesis [22]

iv. Self-Assembly

The self-assembly process is a very complicated method that is only appropriate for lab-scale nanofiber fabrication [19]. As the name implies, self-assembly is a build-up of nanoscale fibers using smaller molecules as fundamental building blocks. Figure 2.4 is a simple representation of self-assembly for acquiring nanofibers [23]. Here, a small molecule (Figure 2.4 top) is organized in a concentric manner such that bonds can form among the concentrically arranged small molecules (Figure 2.4 middle), which, upon expansion in the plane, usually gives the longitudinal axis of a nanofiber (Figure 2.4 bottom). The primary mechanism for general self-

assembly is the intermolecular forces that bring the smaller units together and the structure of the smaller units of molecules that define the shape of the macromolecular nanofiber.

Biomacromolecules' natural driving force drives the molecular self-assembly methods to create functional structures in living beings. Biomacromolecules such as proteins can arrange themselves into various configurations through non-covalent bonding such as hydrogen bonding, van der Waals and hydrophobic interactions. Control of the chemistry behind the natural arrangement of biomacromolecules has resulted in nanofibers' development [24]. For instance, residues of peptides have been chemically altered to produce nanofibers with a hydrophobic interior and hydrophilic exterior diameter of 5 to 8 nm [22].

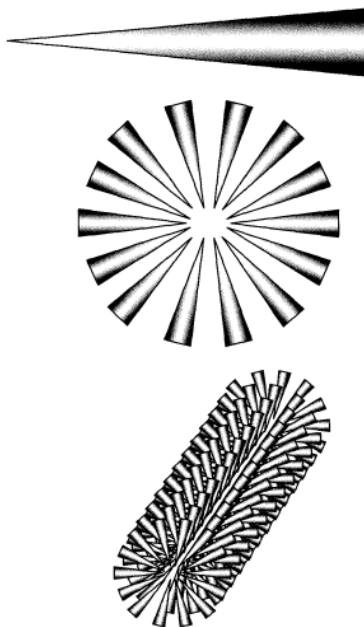


Figure 2. 4 Obtaining nanofibers by self-assembly [23]

v. ***Electrospinning***

Electrospinning is a unique technique for the electrostatic fabrication of polymer nanofibers [25]. Nanofiber production procedures can be commonly categorized into two major categories: (i) physical and chemical production procedures and (ii) electrospinning and non-electrospinning methods. In the bottom-up approach, ions, atoms, molecules, and even nanoparticles can be utilized as the constructing blocks for nanofibers' creation. Top-down methods include

continuous reduction of bulk material by grinding down or milling to generate nanofibers. Electrospinning is the most studied and utilized method to produce nanofibers since the 2000s; however, there are a few challenges. For instance, nanofiber production technique is relatively costly than conventional fibers because of the high cost of technology and the low production rate. The vapors emitted in the electrospinning method cause a health risk. Aside from the electrospinning method, several non-electrospinning procedures were established to improve nanofiber production include solution blowing, template synthesis, drawing methods, phase separation, freeze/drying synthesis, self-assembly, and splitting [26].

One of the more famous procedures to form nanofibers, a style of nanotechnology, is through electrospinning. Electrospinning is the formation of nanofibers using a high electric field. During the 1930s, Antonin Formals' patented electrospinning process presented the possibility for nanofiber production [27] since it could reliably make materials on the nanoscale. Research in the electrospinning field has fundamentally expanded in recent years because of the development of nanotechnology. Vast numbers of the investigations have been conducted in electrospinning to find a way to make various polymers on the nanoscale, and what processing parameters control the electrospinning yield. Despite these advances, electrospinning still seems to be more of artistry than science.

2.3 Comparison of methods for the production of nanofibers

The advantages and disadvantages of the different techniques to produce ultrafine fibers are considered for selection purposes. Even though drawing is the most straightforward approach for creating long fibers, it has a low throughput since fibers are created one at a time. Template synthesis, which needs a nano-porous membrane to form fibrils, cannot generate single continuous long nanofibers. The phase separation and self-assembly techniques could be applied to create nanofibers. However, the planning time is longer than other techniques [28].

Tables 2.1 (a) & (b) compare the different processes for the fabrication of nanofibers.

Table 2. 1 (a) Comparison of processing techniques for obtaining nanofibers

Process	Technological advances	Can the process be scaled?	Repeatability	Convenient to process?	Control on fiber dimensions
Drawing	Laboratory	×	√	√	×
Template Synthesis	Laboratory	×	√	√	√
Phase Separation	Laboratory	×	√	√	×
Self-Assembly	Laboratory	×	√	×	×
Electrospinning	Laboratory (with potential for industrial processing)	√	√	√	√

Table 2. 1 (b) Advantages and disadvantages of various processing techniques

Process	Advantages	Disadvantages
Drawing	Minimum equipment requirement.	Discontinuous process
Template Synthesis	Fibers of different diameters can be easily achieved by using different templates.	Cannot produce long, continuous nanofibers
Phase Separation	Minimum equipment requirement. The process can directly fabricate a nanofiber matrix. Batch-to-batch consistency is achieved easily. The mechanical properties of the matrix can be tailored by adjusting polymer concentration.	Limited to specific polymers
Self-Assembly	Suitable for obtaining smaller nanofibers.	Complex process
Electrospinning	Cost-effective. Long, continuous nanofibers can be produced.	Jet instability

Electrospinning has many advantages over the other four processes and is examined further in section 2.4

2.4 Electrospinning: Working principles and equipment setup

Electrospinning generates fibers with diameters varying from nanometer to micrometer scale when the electrostatic force is used on solutions or melts. The formation of electrospun fibers is based on the uniaxial stretch of viscoelastic solutions. A typical electrospinning arrangement comprises three essential components, as shown in Figure 2.5, namely a high voltage power supply (kV), a syringe with a metallic needle, and a grounded collector. The jetting setup is placed vertically or horizontally and keeps at a certain angle with the collector. The feeding rate

is generally controlled by a syringe pump, which extrudes the needle's solution at a preprogrammed rate. The collector could be a metal plate, a grid, or a roller, depending on the alignment of fibers needed.

The concentration of the polymer solution is critical to the spinning method. Electrospinning of high viscous polymer solution results in fibers with discontinuities. On the other hand, a polymer solution with low viscosity leads to electrospraying instead of electrospinning. In a conventional electrospinning method, high voltage is applied to solutions or melts. A pendant droplet is formed. When the electrostatic repulsion begins to defeat the surface tension of the fluid, the pendant droplet will distort into a conical droplet known as the Taylor cone at the tip of the needle [29]. As the electrostatic force beats the cone-shaped droplet's surface tension, a fine, charged jet stream of the polymer melt is emitted from the needle tip. This affects the jet stream to be elongated continuously as a long and thin filament, and then this filament solidifies and is finally deposited onto a grounded collector, causing the formation of a uniform fiber, as shown in Figure 2.5 [25]. These patterns can help visualize the whipping motion of the jet in the electric field. The dry fibers are collected on the grounded collector in the form of a nonwoven mat. The method is conducted at room temperature, except the heat is needed to keep the polymer in a liquid state. The morphology of the nanofibers is depended on the type of polymer used and the spinning conditions. Fiber fineness can be controlled from ten to a thousand nanometers in diameter [30].

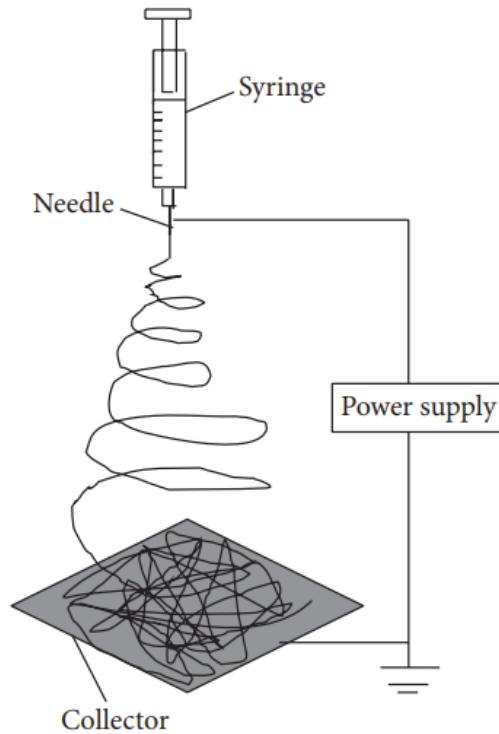


Figure 2. 5 A basic electrospinning device [25]

In the fabrication of electrospun fibers, numerous factors can affect the morphology of electrospun fibers. These factors can be categorized as solution properties, such as viscosity, elasticity, conductivity, and surface tension; control variables, such as electrostatic potential in the capillary, the voltage at the tip of the needle, the distance between the needle and the collector; environmental parameters, such as solution temperature, environment humidity, and temperature, and airflow [28,31].

Electrospinning devices come in various sizes and shapes. The most straightforward kind of electrospinning device consists of a needle with an incorporated wire. The needle can be either metallic or glass. The electrostatic force releases the charged liquid from the needle's tip, producing a jet stream that goes to a grounded collector. Regularly in lab practice, the applied voltage, and the flow rate of the liquid are carefully controlled. A pumping device is utilized to convey the solution to the needle in a more detailed electrospinning gadget. Typically, the solution is fed through a non-conducting tube to the needle to avoid the unwanted electrical discharge from the programmable pumping device. A standard voltage generator delivers 10 to 40 kilovolts at around 100 microamperes of direct current (DC) to the needle through the

electrospinning method. However, an alternating current (AC) generator also works well in electrospinning [32,33], but is rarely selected in research laboratory practice since it is dangerous to the operator. A usual gap between the needle tip and the rotating collector is 10 centimeters or more. The nanofibers collector is available in different patterns. The rotating cylinder is used as a collector for the electrospinning setup.

2.5 Parameters controlling electrospun product form

Many parameters control the product form in electrospinning [34,35]. These parameters can be grouped under three general headings: material parameters, processing parameters, environment parameters [35]. These parameters are summarized in Figure 2.6 and are discussed in more detail in Sections 2.5.1, 2.5.2, and 2.5.3.

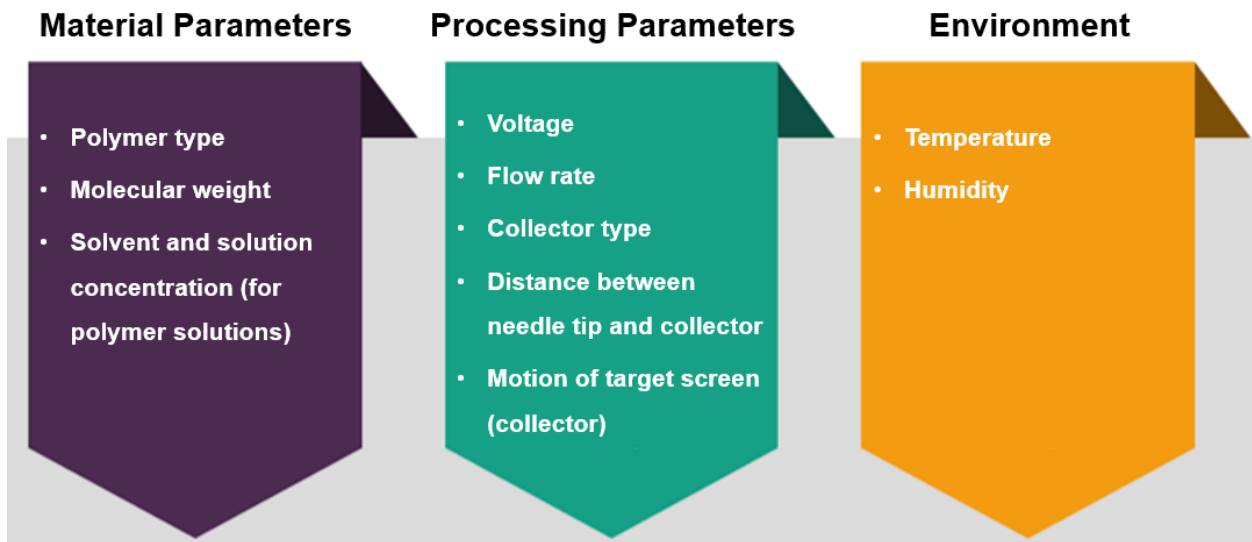


Figure 2. 6 Materials and Processing Parameters

2.5.1 Processing parameters

i. Applied voltage (kV)

The applied voltage to the solution is an essential factor. This is because fiber formation only happens when the applied voltage exceeds the threshold voltage (~ 1 kV/cm, dependent on the polymer solution). In general, applied voltage modifies the nanofiber diameter, but the level of importance differs from other factors such as the polymer solution concentration and the distance between the needle tip and the collector [29,37]. With the increase in applied voltage, the electrostatic force on the solution also increases, which supports extending the jet stream,

eventually decreasing the fiber diameter. It has been discovered that adjusting the applied voltage will modify the initial drop's shape, thus causing a change in the fibers' structure and morphology [38].

ii. Flow rate

The term flow rate is defined as when the polymer solution is pumped into the tip to refill the cone. With a fixed internal diameter of the spinneret, the standard feeding rate is proportionate to the fiber diameter. Preferably, the flow rate must match the pace of the ejection of the polymer solution from the needle tip. Nanofibers of the same diameter are achieved under such conditions. Electrospinning may only be irregular with Taylor's cone being drained at lower flow rates, but at higher flow rates, it results in frequently larger fiber diameters and beads due to not providing enough time for solvent evaporation [39]. Evaporation enhances the flow rate under circumstances where the applied voltage is undoubtedly not a restricting element outcome in the average fiber diameter (nm) [40]. Experimental measurements indicate the volume charge density (qv) on the jet stream is reduced exponentially with flow rate [41]. Higher flow rates probably lower the rate of replacement of charges on the surface of the droplet. Nevertheless, recommended charge renewals be administered by the drift velocity of ions and, hence, free of flow rate [7]. Hence, the lower values of charge density (qv) are expected to result from high rates of withdrawal of charges just as a polymer solution from the droplet surface at the higher flow rates.

iii. Collector

Various collector geometries have been used for electrospinning. These include static plate; parallel plates; rotating disc; rotating drum/mandrel; grid [42, 43]. As noted by Sahay et al. [43], most electrospinning setups that are designed to produce aligned nanofibers employ a rotating device as the collector. The purpose of using a rotating device as the collector is to mechanically stretch the fibers, thereby helping in the alignment of the fibers.

iv. Distance between needle tip to the collector

After the droplets flow from the needle's tip, the solvent evaporates during the time spent traveling to the collector. The polymer reduces or freezes and turns into fibers before collected by the collector. With the increase of the needle tip to collector distance, the flying pathway and

time expand, leading to sufficient fiber diameter, affecting the polymer jet stream's drying process. The nanofibers' diameter and morphology can also be controlled by the gap between the needle tip and the collector, even though the effect is not as prominent as the other earlier indicated parameters [44]. The least distance allows enough time for solvent evaporation before the fibers reach the collector is needed in electrospinning. Long-distance has generated thinner fibers. Beads are produced when the distance was excessively far or excessively close [31,35].

Short distances will limit the polymer jet stream's drying, probably affecting wet and/or thick nanofibers. Longer distances reduce the electric field intensity between the nozzle and the collector, obstructing a jet stream's development at the needle tip. To overcome this difficulty, the voltage applied will have to be increased. In general, the spinneret-collector distance should be adjusted for a specific polymer solution to allow the solidification and stretching of the polymer jet, which is necessary to create thin and dried fibers [45].

2.5.2 Materials Parameters

i. Molecular weight

As noted by Bhardwaj and Kundu [32] and Haghi and Akbari [36], the molecular weight of the polymer has a significant effect on both the rheological (viscosity, surface tension) and electrical (conductivity, dielectric strength) properties of the polymer solution and, therefore, the electrospun product form.

Bhardwaj and Kundu [32], in their extensive review of electrospinning, conclude that high molecular weight polymer solutions have been generally used in electrospinning since they provide the desired viscosity for fiber generation.

Low molecular weight solutions tend to form beads or beaded fibers [46-51]. The formation of beads or beaded fibers has been related to the instability of the jet of the polymer solution [52, 53].

When fibers are formed, higher molecular weight solutions tend to form fibers with a larger average diameter [36]. Koski et al. [54], in their studies on electrospinning PVA, found that the fiber diameter increases with both molecular weight and concentration. They also found that the

fibers morphology changes from a circular cross-section to flat fibers at high molecular weight and concentration [54].

With respect to the molecular weight of polymers, another factor to consider is dispersity. A uniform polymer is composed of molecules of the same mass. In a disperse (non-uniform) polymer, the chain lengths vary over a range of molecular masses. Human-made (synthetic) polymers are typically dispersed. The dispersity, formally known as the polydispersity index (PDI), is a measure of the distribution of molecular mass in a sample. PDI can be calculated using equation (2.1) [55]:

$$\mathbf{PDI = Mw/Mn} \qquad \mathbf{Equation 2.1}$$

where Mw is the weight average molecular weight, and Mn is the mass average molecular weight. Such variations in PDI can affect the viscosity of solutions made from polymers with the same "nominal" average molecular weight.

ii. Solvent

The selection of solvent [56] mainly defines:

- The spatial arrangement of the atoms in a molecule of the broke down polymer chains
- Ease of charging the spinning jet
- The cohesion of the solution due to surface tension forces
- Rate of solidification of the polymer jet stream on evaporation of the solvent

Dissimilar with droplets of low-molecular-weight solution or monomers divided into smaller droplets under a strong electric field, polymer solutions go through a level of elongational flow and alignment in an electric field [28]. It is the entanglement of the moderately aligned, enlarged conformations of polymer chains that produce their electrospinning workable in any case. Solvents that generate open configurations of polymer chains and high-solids substances are more appropriate for electrospinning [57]. The average nanofiber diameters d (nm) found on electrospinning differed broadly with the solvent utilized, and thinner fibers were achieved with solvents with higher dielectric constant [30].

iii. Solution concentration

Solution concentration is one of the reasons that determine the diameter of nanofibers [34,40]. It has been discovered that fibers with a smaller diameter can be achieved by decreasing the polymer mixture's solution concentration. In any case, when the solution concentration is reduced to the entanglement concentration (C_e), beaded nanofibers are generated [36]. Below the entanglement concentration (C_e), just beaded nanofibers are formed due to the absence of entanglement structure. A rise in a solution concentration above the entanglement concentration (C_e) inhibits the creation of beaded nanofibers, and at 2–2.5 times, the entanglement concentration (C_e) defect-free nanofibers are formed. When the solution concentration is excessively high, ribbon-like structures are created [58].

2.5.3 Environmental Parameters

i. Temperature

An electrospinning procedure relies significantly on the polymer's rheological property, the solution, and the solvent's vapor pressure. The room temperature affects both the rheology of a solution and the solvent's vapor pressure.

ii. Relative Humidity

As noted by Nezerati et al. [59], although environmental factors such as humidity can have a strong impact on fiber morphology, humidity values are often not reported in the literature. This makes the comparison between different studies difficult, if not impossible. Nezerati et al. [59] further noted that "contradictory effects have been observed that appear to be dependent on properties such as the type of polymer, polymer-solvent combination, molecular weight, polymer hydrophilicity and size of the electrospun structure". Aguirre-Chagala et al. [60] agree that the effect of relative humidity has not been sufficiently investigated.

De Vrieze et al. [61] have shown that the relative humidity can affect the fiber structure and dimensions and that the electrospinning process is more difficult at high humidity. For water-based solvents, thinner polymer fibers have been observed at higher relative humidity, and vice-versa [62, 63]. For non-water based solvents, the effects of relative humidity on the electrospun fiber morphology are, at least partially, dependent on solvent miscibility with water [59]. Other studies [64] have shown that the surface morphology of the fibers is dependent on the relative

humidity: increasing humidity causes an increase in the number, diameter, shape, and distribution of surface pores. Such surface features may allow fibers to be customized for specific uses in filtration, tissue engineering, and drug delivery [40,64].

2.6 Polyethylene Oxide (PEO)

Electrospinning of polyethylene oxide (PEO) has been analyzed in detail by many scholars. It is soluble in a series of solvents such as water, dimethylformamide (DMF), ethanol, and chloroform [65]. Biocompatibility and non-toxicity are two essential properties that represent PEO as a suitable biomaterial for application in areas such as tissue engineering and wound scaffolds. PEO has helped as an ideal applicant to increase a vital understanding of the outcomes of numerous parameters during electrospinning such as applied voltage, solution concentration, flow rate, the distance between the needle tip to the collector, and solution properties such as intrinsic viscosity and entanglement number. It indicates that solution properties perform a vital role in the formation and morphology of resulting nanofibers [66]. The adaptability of PEO in electrospinning has been crucial in the processing of polymers that cannot be electrospun on their own such as chitosan, proteins, alginate, and hyaluronan [67].

Among the polymers that have been examined in electrospinning research, PEO is the one that has been most well-characterized due to its attractive properties that provide for ease of electrospinning. Chemically, PEO is like poly (ethylene glycol) (PEG), except that PEO has a higher molecular weight. When the molecular weight is lower than 20 kDa, the polymer is generally recognized as PEG [68]. PEO is a linear polymer that comprises ethylene and ether segments $[-CH_2CH_2O-]_n$ (where n , the degree of polymerization ranges from 2000 to 100,000 [69]). The ether oxygen permits this polymer to mix with other hydrophilic species, while the ethylene part joins in hydrophobic interactions. Due to its amphiphilic nature, PEO is soluble in water by forming hydrogen bonding among the PEO ether group's oxygen and the hydrogen of water molecules [70]. Also, the oxygen-oxygen inter distance on the PEO backbone matches the oxygen atoms (2.8 \AA) in the water molecules, which is vital in making the polymer soluble in water. Homologues of PEO, such as poly (methyl ethylene) and poly (propyl ethylene), are not water-soluble due to the mismatch oxygen-oxygen inter distance with that of water [71].

Numerous researchers have studied the unique properties of PEO in water. Hydration of PEO creates a cage that protects the hydrophobic ethylene parts from the hydrophilic environment. Two to three molecules of water are required to hydrate a PEO monomer segment [69,72, C1]. Cluster formation has been observed in dilute aqueous solutions of PEO.

Hammouda et al. [72] found that cluster formation is driven by hydrophobic forces between the PEO chain's methyl groups, and higher levels of polymer concentration had a higher tendency to form clusters. Figure 2.7 is a schematic of PEO clustering in water due to the end chain effect [72]. Bekiranov et al. [68] observed that PEO did not cluster in water for polymers with molecular weights varying from 8kDa to 4000 kDa. They speculated that the hydrophilic forces of PEO decreased as the molecular weight decreased [68]. The temperature has also been reported to affect the formation of clusters in aqueous solutions of PEO [74, 75, 76]. With an increase in temperature, the entropy of a PEO aqueous solution is also higher, supporting hydrophobic forces between PEO molecules but decreasing contact between PEO and water [74]. The attractive entropic interaction in an aqueous solution of PEO increases as the temperature increases, even though the enthalpic repulsive interaction increases as the temperature decreases [75]. Israelachvili [76] asserts that short-chain PEO is truly water-soluble in the temperature range from 25 to 75°C. Devanand and Selser [77] also suggest no aggregation (clusters) for PEO in water.

Hammoudi et al. [72] explained the effects of chain-end on PEO clustering in organic solvents. When both ends of the PEO chain are methyl groups (-OCH₃), PEO can be completely dissolved in benzene. On the other hand, when both ends of the PEO chain are hydroxyl groups (-OH), which resist benzene, they are drawn to oxygen in the polymer chain. In methanol, the effect of chain-end is insignificant, as methanol (CH₃-OH) has both a hydrophobic and a hydrophilic group, and PEO is soluble in methanol [72].

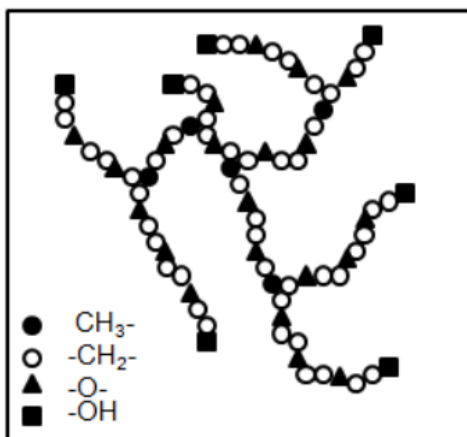


Figure 2.7 Schematic representation of PEO clustering in water due to end chain effect [72]

2.7 Electrospinning of PEO

The electrospinning of PEO has been examined by numerous researchers over the years.

A classic paper in 1995 by Doshi and Reneker [31] describes the electrospinning process, the processing conditions, fiber morphology, and some possible uses of electrospun fibers in agriculture, medical, and composite areas. PEO was used as a "model" material for these studies. The PEO used had a molecular weight of 1,450,000 g/mol. By adjusting the concentration of PEO in water, and other processing conditions, fibers with a variety of cross-sectional shapes and sizes were produced. The diameter of the fibers varied from 50nm to 5 microns. The diameter of the fibers could be adjusted by changing such processing parameters as an electric field, the distance between the needle tip and collector, and the viscosity of the solution. Fibers were only formed at viscosities between 800 and 4000 cP. The cross-sectional shape of these fibers was usually circular, but sometimes the fibers had sections with "beads".

The formation of beaded fibers has been widely observed, including in nature with spider silk [78]. Jaeger et al. [79, 80] were one of the first research groups to examine electrospun fibers obtained from aqueous solutions of PEO. They found that there was a relationship between the bead diameter and spacing and the fiber diameter. The smaller the fiber diameter, the smaller was the bead diameter, and the shorter was the distance between the beads.

Reneker and his group [58] followed up their earlier work on beaded fibers in PEO with a more extensive examination which looked at changing the solvent. PEO with an average molecular

weight of 900,000 g/mol was used for the study, and three series of solutions were used, namely: PEO with distilled water only; PEO and NaCl with distilled water; PEO with distilled water and ethanol. They found that the viscoelasticity of the solution, charge density carried by jet, and the surface tension of the solution are the key factors that influence the formation of beaded fibers. By changing the solvent from pure water to a water/ethanol mixture for a fixed PEO concentration, smoother fibers with larger diameters were produced. The addition of NaCl helps in preventing the formation of beads. They were successful in forming bead-free fibers with diameters in the range of 100 nm.

In 2001, there was a series of papers by Hohman et al. [81,82,83,84] that examined the electrospinning process and the role of jet instabilities on the production of nanofibers. They attempted to understand how the electrospinning process transforms a millimeter-diameter fluid stream into solid fibers four orders of magnitude smaller in diameter. All experimental work was conducted with PEO (molecular weight 2,000,000 g/mol) and aqueous solutions. Their studies showed that the most important element operative during electrospinning is the rapid growth of a "whipping" instability that causes bending and stretching of the jet.

In terms of understanding the electrospinning of PEO, the seminal and highly cited paper by Deitzel et al. [29] is of major significance. All experiments were performed with a PEO of molecular weight of 400,000 g/mol and aqueous solutions with PEO concentrations ranging from 4 to 10%. They found that the morphology of the nanofibers produced was strongly influenced by processing parameters (feed rate, voltage) and solution parameters (concentration, viscosity, surface tension). An increasing number of bead defects was correlated to a decrease in the stability of the jet as the voltage is increased. The properties of the PEO solutions defined the processing window and influenced the size and distribution of the nanofibers. Fibers could be electrospun from solutions containing 4 to 10wt% PEO. The diameter of the fibers was found to increase with solution concentration according to a power law relationship. Deitzel et al. [85] followed up their original study with a paper that characterized the fibers using wide-angle x-ray diffraction, optical microscopy, and environmental scanning microscopy.

Reneker et al. [86] examined the effects of humidity on the electrospinning of PEO. PEO with a molecular weight of 400,00 g/mol was used, and an aqueous solution containing 6wt% PEO. The

relative humidity was varied between 5.1 and 63.5%. As the relative humidity increased from 5.1% to 48.7%, the fiber diameter decreased from 253nm to 144nm. When the relative humidity increased above 50%, beaded fibers were formed.

Shenoy et al. [87], using previously published data for PEO [84,85, 29] and entanglement (Me) and weight average (Mw) molecular weights, formulated a semi-empirical analysis whereby the required polymer concentration for fiber formation may be determined a priori. Processing regions could be defined where beads, fibers+ beads, or fibers only, were formed. They also pointed out that for low molecular weight polymer, it was challenging to obtain fibers, even at high concentrations.

Son et al. [44] investigated the electrospinning of PEO (molecular weight 300,000 g/mol) in solutions of water, ethanol, dimethylformamide (DMF), and chloroform. The weight percent PEO in solution required to form fibers varied with the solvent: chloroform (4.0wt%); Ethanol (4.0wt%); DMF (7.0wt%); Water (7.0wt%). Fiber formation was related to the intrinsic viscosity.

Using PEO as the "model" material, Agic [88] has modeled the electrospinning process and jet instabilities and correlated the analysis with experimental data on fiber formation and fiber diameter.

Although PEO has easy spinnability, many other polymeric materials cannot be electrospun in their pure form. However, as noted by Filip and Peer [89], even small quantities of PEO, often less than 2%, render these materials electrospinnable. Examples of polymeric materials that can be electrospun with small additions of PEO include poly(N-isopropylacryamide), a carrier for controlled drug release [90]; poly (ethylene terephthalate), PET [91]; urea [92]; chitosan [93]; keratin [94]; pectin [95].

2.8 References

1. Roco, M.C. Nanotechnology: convergence with modern biology and medicine. *Current Opinion in Biotechnology*, Vol. 14, No. 3, pp. 337–346, (2003).
2. Zhang, L., Chae, S.R., Hendren, Z., Park, J.S., and Wiesner, M. R. "Recent advances in proton exchange membranes for fuel cell applications," *Chemical Engineering Journal*, Vol. 204-205, pp. 87–97, (2012).
3. Kumar, G. G., and Nahm, K. S. "Polymer nanocomposites fuel cell applications," in *Advances in Nanocomposite-Synthesis, Characterization and Industrial Applications*, pp. 639–660, Intech Europe, Vienna, Austria, 2011.
4. Luzio, A., Canesi, E.V., Bertarelli, C., and Caironi, M., Electrospun polymer fibers for electronic applications, *Materials*, Vol. 7, pp. 906-947, (2014).
5. Feynman, Richard P. There is plenty of room at the bottom. *Engineering and Science*, Vol. 23, No. 5, pp. 22-36, (1960).
6. Murat, S., Zakir, R., and Ulviya, B. Multifunctional electroactive electrospun nanofiber structures from water solution blends of PVA/ODA-MMT and poly (maleic acid- alt acrylic acid): effects of Ag, organoclay, structural rearrangement, and NaOH doping factors. *Advances in Natural Sciences: Nanoscience and Nanotechnology*, Vol. 7, No. 2, pp. 1–13, (2016).
7. Theron, S., Yarin, A., Zussman, E., and Kroll, E. Multiple jets in electrospinning: experiment and modeling. *Polymer*, Vol. 46, No. 9, pp. 2889–2899, (2005).
8. Venugopal, J., and Ramakrishna, S. Applications of polymer nanofibers in biomedicine and biotechnology. *Applied Biochemistry and Biotechnology*, Vol. 125, pp. 147-157, (2005).
9. Martins, A., Araujo, J. V., Reis, R. L., and Neves, N. M. Electrospun nanostructured scaffolds for tissue engineering applications, *Nanomedicine*, Vol. 2, No. 6, pp. 929–942, (2007).

10. Schreuder-Gibson H.L., Truong Q., Walker J.E., Owens J.R., Wander J.D., Jones W.E., Chemical, and Biological Protection and Detection in Fabrics for Protective Clothing, *Material Research Society Bulletin*, Vol. 28, pp. 574-578, (2003).
11. Stitzel, J.D., Bowlin, G.L., Mansfield, K., Wnek, G.E., and Simpson, D.G. Tailoring tissue engineering scaffolds using electrostatic processing techniques: a study of poly (glycolic acid) electrospinning, 32nd SAMPE Meeting, Boston, pp. 205-211, (2000).
12. Cowan, K., and Gogotsi, Y. The Drexel/UPenn IGERT: Creating a new model for graduate education in nanotechnology. *The Journal of Materials Education*, Vol. 26, pp. 147-152, (2004).
13. Ondarcuhu, T., and Joachim, C. Drawing a single nanofiber over hundreds of microns. *Europhysics Letters*, Vol. 42, No. 2, pp. 215-220, (1998).
14. Jayaraman, K., Kotaki, M., Zhang, Y., Mo, X., and Ramakrishna, S. Recent advances in polymer nanofibers. *Journal of Nanoscience and Nanotechnology*, Vol. 4, No. 2, pp. 52 - 65, (2004).
15. Sarbatly, R., Krishnaiah, D., and Kamin, Z. A review of polymer nanofibres by electrospinning and their application in oil-water separation for cleaning up marine oil spills. *Marine Pollution Bulletin*, Vol. 106, No. 1, pp. 8-16, (2016).
16. Alberts, B., Johnson, A., Lewis, J., Raff, M., Roberts, K., and Walter, P. *Molecular Biology of the Cell*. 4th edition. New York: Garland Science; 2002. DNA Replication Mechanisms.
17. Feng, L., Li, S.H., Li, H.J., Zhai, J., Song, Y.L., Jiang, L., and Zhu, D.B. Super-hydrophobic surface of aligned polyacrylonitrile nanofibers. *Angewandte Chemie International Edition*, Vol. 41, No. 7, pp. 1221-1223, (2002).
18. Martin, C.R. Template synthesis of electronically conductive polymer nanostructures. *Accounts of Chemical Research*, Vol. 28, No. 2, pp. 61-68, (1995).

19. Malkar, N.B., Lauer-Fields J.L., Juska, D., and Fields, G.B. Characterization of peptide amphiphiles possessing cellular activation sequences. *Biomacromolecules*, Vol. 4, No. 3, pp. 518-528, (2003).
20. Lloyd, D. R., Kinzer, K. E., and Tseng, H. S. Microporous membrane formation via thermally induced phase separation. I. Solid-liquid phase separation. *Journal of Membrane Science*, Vol. 52, pp. 239, (1990).
21. Heijkants, R. G. J. C., Tienen, T. G. V., Groot, J. H. D., Pennings, A. J., Buma, P., Veth, R. P. H., and Schouten, A. J. Preparation of polyurethane scaffold for tissue engineering made by a combination of salt leaching and freeze-drying of dioxane. *Journal of Materials Science*, Vol. 41, pp. 2423-2428, (2006).
22. Vasita, R., and Katti, D.S. Nanofibers and their applications in tissue engineering. *International Journal of Nanomedicine*, Vol. 1, No. 1, pp:15-30, (2006).
23. Hartgerink, J.D., Beniash, E., and Stupp, S.I. Self-assembly and mineralization of peptide-amphiphile nanofibers. *Science*, Vol. 294, No. 5547, pp. 1684-1688, (2001).
24. Zhang, S., 2003. Fabrication of novel biomaterials through molecular self-assembly. *Nature Biotechnology*, Vol. 21, No. 10, pp. 1171- 1178, (2003).
25. Bognitzki, M., Czado, W., Frese, T., Schaper A., Hellwig M., Steinhart M., Greiner A., and Wendorff J. H., *Nanostructured Fibers Via Electrospinning Advanced Materials*, Vol. 13, pp. 70-72, (2001).
26. Ellison, C. J., Phatak, A., Giles, D.W., Macosko, C.W., Bates, F. S. Melt blown nanofibers: fiber diameter distributions and onset of fiber breakup. *Polymer*, Vol. 48, pp. 3306–3316, (2007).
27. Formhals, A. Process and apparatus for preparing artificial threads, U.S. Patent 1975504, 1934.
28. Huang, Z.M., Zhang, Y.Z., Kotaki, M., Ramakrishna, S. Review of polymer nanofiber by electrospinning and their applications in nanocomposites. *Composites Science Technology*, Vol. 63, pp. 2223-2253, (2003).

29. Deitzel, J.M., Kleinmeyer, J., Harris, D., and Beck Tan, N.C. The effect of processing variables on the morphology of electrospun nanofibers and textiles, *Polymer*, Vol. 42, pp. 261–272, (2001).
30. Subbiah, T. Electrospinning of nanofibers, *Journal of Applied Polymer Science*, Vol. 96, pp. 557–69, (2005).
31. Doshi, J., and Reneker, D.H. Electrospinning process and applications of electrospun fibers, *Journal of Electrostatics*, Vol. 35, pp. 151–160, (1995).
32. Bhardwaj, N., and Kundu, S. C. Electrospinning: a fascinating fiber fabrication technique, *Biotechnology Advances*, Vol. 28, No. 3, pp. 325–347, (2010).
33. Kessick, R., Fenn, J., and Tepper, G. The use of AC potentials in electrospraying and electrospinning processes. *Polymer*, Vol. 45, pp. 2981-2984, (2004).
34. Almetwally, A.A., El-Sakhawy, M., Elshakankery, M.H., and Kasen, M.H., Technology of nanofibers: production techniques and properties- a critical review, *Journal of the Textile Association*, Vol. 78, No. 1, pp. 5-14, (2017).
35. Salas, B. Solution electrospinning of nanofibers. In: *Electrospun Nanofibers*, Ed. Mehdi Afshari, Cambridge, UK: Woodhead Publishing, pp. 73-108, (2016).
36. Haghi, A. K., and Akbari, M. Trends in electrospinning of natural nanofibers, *Physica Status Solidi (A) Applications and Materials*, Vol. 204, No. 6, pp. 1830–1834, (2007).
37. Pawlowski, K. J., Barnes, C. P., Boland, E. D., Wnek, G. E., and Bowlin, G. L. Biomedical nanoscience: electrospinning basic concepts, applications, and classroom demonstration, *Materials Research Society Symposium Proceedings*, Vol. 827, pp. 17–28, (2004).

38. Buchko, C. J., Chen, L. C., Yu, S., Martin, D. C. Processing, and microstructural characterization of porous biocompatible protein polymer thin films. *Polymer*, Vol. 40, pp. 7397-7407, (1999).
39. Megelski, S., Stephens, J. S., Chase, D. B., Rabolt, J. F. Micro and nanostructured surface morphology on electrospun polymer fibers. *Macromolecules*, Vol. 35, pp. 8456-8466, (2002).
40. Greiner, A., and Wendorff, J. H. Electrospinning: a fascinating method for the preparation of ultrathin fibers, *Angewandte Chemie*, Vol. 46, No. 30, pp. 5670–5703, (2007).
41. Shin, Y.M., Hohman, M.M., Brenner, M.P., and Rutledge, G.C. Experimental characterization of electrospinning: the electrically forced jet instabilities. *Polymer*, Vol. 42, pp. 9955-9967, (2001).
42. Zander, N.E. Hierarchically structured electrospun fibers. *Polymers*, Vol. 5, pp. 19-44, (2013).
43. Sahay, R., Thavasi, V., and Ramakrishna, S., Design modifications in electrospinning setup for advanced applications. *Journal of Nanomaterials*, Article ID 317673, pp. 1-17, (2011).
44. Son, W. K., Youk, J. H., Lee, T. S., and Park, W. H. The effects of solution properties and polyelectrolyte on electrospinning of ultrafine poly (ethylene oxide) fibers, *Polymer*, Vol. 45, pp. 2959-2966, (2004).
45. Ying, Y., Zhidong, J., Qiang, L., and Zhicheng, G. Experimental investigation of the governing parameters in the electrospinning of polyethylene oxide solution, *IEEE Transactions on Dielectrics and Electrical Insulation*, Vol. 13, pp. 580-585, (2006).
46. Kim, W.K., Lee, K.H., Khil, M.S., Ho, Y.S., and Kim, H.K., The effect of molecular weight and linear velocity of drum surface on the properties of electrospun poly (ethylene terephthalate) nonwovens, *Fibers and Polymers*, Vol. 5, No. 2, pp.122-127, (2004).

47. Colmenares-Roldan, G.J., Quintero-Martinez, Y., Aguldelo-Gomez, L.M., Rodriguez-Vinasco, L.F., and Hoyos-Palacio, L.M. Influence of the molecular weight of polymer, solvents and operational condition on the electrospinning of polycaprolactone, *Revista Facultad de Ingenieria, Universidad de Antioquia*, Vol. 84, pp. 35-45, (2017). DOI: 10.17533/udea.redin.n84a05
48. Gupta, P., Elkins, C., Long, T.E., and Wilkes, G.I. Electrospinning of linear homopolymers of poly(methyl methacrylate): exploring relationships between fiber formation, viscosity, molecular weight and concentration in a good solvent, *Polymer*, Vol. 46, pp. 4799-4810, (2005).
49. Tan, S.H., Inai, R., Kotaki, M., and Ramakrishna, S. Systematic parameter study for ultra-fine fiber formation via electrospinning process, *Polymer*, Vol. 46, pp. 6128-6134, (2005).
50. Chen, Z., Ma, X., and Qing, F. Electrospinning of collagen-chitosan complex, *Materials Letters*, Vol. 61, pp.3490-3494, (2007).
51. Haider, A., Haider, S., and Kang, I.K. A comprehensive review summarizing the effect of electrospinning parameters and potential applications of nanofibers in biomedical and biotechnology, *Arabian Journal of Chemistry*, Vol. 11, pp. 1165-1188, (2018).
52. Yarin, A.L. *Free liquid jets, and films: hydrodynamics and rheology*, New York: Wiley, 1993.
53. Entov, V.M., and Shmaryan, L.E. Numerical modeling of the capillary breakup of jets of polymer liquids, *Fluid Dynamics*. Vol. 32, No. 5, pp. 696-703, (1997).
54. Koski, A., Yim, K., and Shivkumar, S. Effect of molecular weight on fibrous PVA produced by electrospinning, *Materials Letters*, Vol. 58, pp. 493-497, (2004).
55. Stepto, R.F.T., Gilbert, R.G., Hess, M., Jenkins, A.D., Jones, R.G., and Kratochvil, P. Diversity in polymer science, *Pure and Applied Chemistry*, Vol. 81, No. 2, pp. 351-353, (2009).

56. Venugopal, J., Zhang, Y. Z., and Ramakrishna, S. Electrospun nanofibers: biomedical applications, *Proceedings of the Institution of Mechanical Engineers*, Vol. 218, pp. 35–45, (2005).
57. Ramakrishna, S., Fujihara, K., Teo, W.E., Lim, T.C., and Ma, Z. *An Introduction to Electrospinning and Nanofibers*, World Scientific, Singapore, 2005.
58. Fong, H., Chun, I., and Reneker D. H. Beaded nanofibers formed during electrospinning. *Polymer*, Vol. 40, pp. 4585–4592, (1999).
59. Nezerati, R.M., Eifert, M.B., and Cosgriff-Hernandez, E. Effects of humidity and solution viscosity on electrospun fiber morphology. *Tissue Engineering (Part C)*, Vol. 19, No. 10, pp 810-819, (2013).
60. Aguirre-Chagala, Y.E., Altuzar-Aguilar, V.M., Dominguez-Chavez, J.G., Rubio-Cruz, E.F., and Mendoza-Barrera, C.O. Influence of relative humidity on the morphology of electrospun polymer composites. *Der Chemica Sinica*, Vol. 8, No. 1, pp 83-92, (2017).
61. De Vrieze, S., Van Camp, T., Nelvig, A., Hagstrom, B., and Westbrock, P., The effect of temperature and humidity on electrospinning. *Journal of Materials Science*, Vol. 44, pp. 1357-1362, (2009).
62. Pelipenko, J., Kristl, J., Jankovic, B., Baumgartner, S., and Kocbek, P. The impact of relative humidity during electrospinning on the morphology and mechanical properties of nanofibers. *International Journal of Pharmaceutics*, Vol. 456, pp. 125-134, (2013).
63. Huang, I.W., Bui, N.N., Manickam, S.S., and McCutcheon, J.R. Controlling electrospun nanofiber morphology and mechanical properties using humidity. *J. Polymer Science (Part B: Polymer Physics)*, Vol. 49, pp.1734-1744, (2011).
64. Casper, C.L., Stephens, J.S., Tassi, N.G., Chase, D.B., and Rabolt, J.F. Controlling surface morphology of electrospun polystyrene fibers: effect of humidity and molecular weight in the electrospinning process. *Macromolecules*, Vol. 37, pp. 573-578, (2004).

65. Hutmacher, D. W., and Dalton, P. D. Melt electrospinning, *Chemistry: An Asian Journal*, Vol. 6, pp. 44-56, (2011).
66. Thompson, C. J., Chase, G. G., Yarin, A. L., and Reneker, D. H. Effects of parameters on nanofiber diameter determined from electrospinning model. *Polymer*, Vol. 48, pp. 6913-6922, (2007).
67. Brandrup, J., and Immergut, E.H. *Polymer Handbook*, 2nd ed., John Wiley & Sons Inc., New York, (1975).
68. Bekiranov, S., Bruinsma, R., and Pincus, P. Solution behavior of poly (ethylene oxide) in water as a function of temperature and pressure. *Physical Review E*, Vol. 55, pp. 577-585, (1996).
69. Maxfield, J., and Shepherd, I. W. Conformation of poly (ethylene oxide) in the solid-state, melt, and solution measured by Raman scattering. *Polymer*, Vol. 16, pp. 505-509, (1975).
70. Reneker, D. H., and Chun, I. Nanometer diameter fibers of polymer, produced by electrospinning, *Nanotechnology*, Vol. 7, No. 3, pp. 216–223, (1996).
71. Ji, Y., Ghosh, K., Shu, X.Z., Li, B., Sokolov, J.C., Prestwich, G.D., Clark, R.A.F., and Rafailovich, M.H. Electrospun three- dimensional hyaluronic acid nanofibrous scaffolds. *Biomaterials*, Vol. 27, pp. 3782-3792, (2006).
72. Hammouda, B., Ho, D. L., and Kline, S. Insight into clustering in poly (ethylene oxide) solutions. *Macromolecules*, Vol. 37, pp. 6932-6937, (2004).
73. Dahal, U.R., and Dormidontova, E.E. The dynamics of solvation dictates the conformation of polyethylene oxide in aqueous, isobutyric acid and binary solutions, *Physical Chemistry Chemical Physics*, Vol. 19, pp. 9823-9832, (2017).
74. Polverari, M., and Van de Ven, T. G. M. Dilute aqueous poly (ethylene oxide) solutions: Clusters and single molecules in thermodynamic equilibrium. *Journal of Physical Chemistry*, Vol. 100, pp. 13687-13695, (1996).

75. Faraone, A., Magazu, S., Maisano, G., Migliardo, P., Tettamanti, E., and Villari, V. The puzzle of poly (ethylene oxide) aggregation in water: Experimental findings. *Journal of Chemical Physics*, Vol.110, pp. 1801-1806, (1999).
76. Israelachvili, J. The different faces of poly (ethylene glycol). *Proceedings of National Academy of Sciences, USA*, Vol. 94, pp. 8378-8379, (1997).
77. Devanand, K., and Selser, J.C. Polyethylene oxide does not necessarily aggregate in water. *Nature*, Vol. 343, pp. 739-741, (1990).
78. Vollrath, F., and Edmonds, D.T. Modulation of the mechanical properties of spider silk by coating with water, *Nature*, Vol. 340, No. 27, pp. 305-307, (1989).
79. Jaeger, R., Schonherr, H., and Vancso, G.J. Chain packing in electrospun poly (ethylene oxide) visualized by atomic force microscopy, *Macromolecules*, Vol. 29, pp. 7634-7636, (1996).
80. Jaeger, R., Bergshoef, M.M., Batlle, C.M., Schonherr, H., and Vancso, G.J. Electrospinning of ultra-thin polymer fibers, *Macromolecular Symposium*, Vol. 127, pp. 141-150, (1998).
81. Shin, Y.M., Hohman, M.M., Brenner, M.P., and Rutledge, G.C. Electrospinning: a whipping jet generates submicron polymer fibers. *Applied Physics Letters*, Vol. 78, No. 8, pp. 1149-1151, (2001).
82. Hohman, M.M., Shin, M., Rutledge, G., and Brenner, M.P. Electrospinning, and electrically forced jets I Stability theory, *Physics of Fluids*, Vol. 13, pp. 2201-2220, (2001).
83. Hohman, M.M., Shin, M., Rutledge, G., and Brenner, M.P. Electrospinning and electrically forced jets, II Applications, *Physics of Fluids*, Vol.13, pp.2221-2236, (2001).
84. Shin, Y.M., Hohman, M.M., Brenner, M.P., and Rutledge, G.C. Experimental characterization of electrospinning: The electrically forced jet and instabilities, *Polymer*, Vol. 42, No. 25, pp. 9955-9967, (2001).

85. Deitzel, J.M., Kleinmeyer, J., Hirvonen, J.K., and Beck Tan, N.C. Controlled deposition of electrospun poly (ethylene oxide) fibers, *Polymer*, Vol. 42, pp. 8163-8170, (2001).
86. Tripatanasuwan, S., Zhong, Z., and Reneker, D.H. Effect of evaporation and solidification of the charged jet in electrospinning of poly (ethylene oxide) aqueous solution, *Polymer*, Vol. 48, pp. 5742-5746, (2007).
87. Shenoy, S.L., Bates, W.D., Frisch, H.L., and Wnek, G.E. Role of chain entanglements on fiber formation during electrospinning of polymer solutions: good solvent, non-specific polymer-polymer interaction limit, *Polymer*, Vol. 46, pp. 3372-3384, (2005).
88. Agic, A. Electrospinning: theoretic foundations and processing parameters, *Polimeri (Zagreb)*, Vol. 25, No. 4, pp. 116-121, (2004).
89. Filip, P., and Peer, P. Characterization of poly (ethylene oxide) nanofibers – mutual relations between mean diameter of electrospun nanofibers and solution characteristics. *Processes*, Vol. 7, No. 948, pp. 1-9, (2019).
90. Song, F., Wang, X.L., and Wang, Y.Z. Poly (N-isopropyl acrylamide/poly (ethylene oxide) blend nanofibrous scaffolds. *Colloids and Surfaces B: Biointerfaces*, Vol. 88, pp. 749-754, (2011).
91. Phaneuf, M.D., Bide, M.J., Bachuwar, A., Mignanelli, M., and Brown, P.J. Production, and selected properties of electrospun poly (ethylene terephthalate) nanofibers. *AATCC Review*, Vol. 7, No. 3, pp. 40-45, (2007).
92. Liu, Y., and Pellerin, C. Highly oriented electrospun fibers of self-assembled inclusion complexes of poly (ethylene oxide) and urea. *Macromolecules*, Vol. 39, No.26, pp. 8886-8888, (2006).
93. Pakravav, M., Heuzey, M.C, and Ajj, A. A fundamental study of chitosan/PEO electrospinning. *Polymer*, Vol. 52, pp. 4813-4824, (2011).

94. Aluigi, A., Vineis, C., Varesano, A., Mazzuchetti, G., Ferrero, F., and Tonin, C. Structure, and properties of keratin/PEO blend nanofibers. *European Polymer Journal*, Vol. 44, pp. 2465-2475, (2008).
95. Akinalan Balik, B., and Argin, S. Role of rheology on the formation of nanofibers from pectin and polyethylene oxide blends. *Journal of Applied Polymer Science*, Vol. 137, No. 3, art.no. 48294, (2020).

CHAPTER 3

EXPERIMENTAL DETAILS

This chapter is divided into several sections/sub-sections.

Section 3.1 gives details of the design and construction of purpose-built electrospinning equipment used for the exploratory study of the effect(s) of material and processing parameters on the production of nanofibers of PEO.

Section 3.2 describes the experimental details for the exploratory study. This section has four sub-sections, namely:

3.2.1 Materials (PEO and solvents) used.

3.2.2 Preparation of solutions for electrospinning.

3.2.3 Operating procedures for electrospinning.

3.2.4 Preparation and characterization of the electrospun product using optical microscopy (OM), scanning electron microscopy (SEM), and image analysis.

3.1 Design and Construction of Purpose-built Electrospinning Equipment

Figure 3.1 shows the electrospinning system that was purpose-built for use in this study.

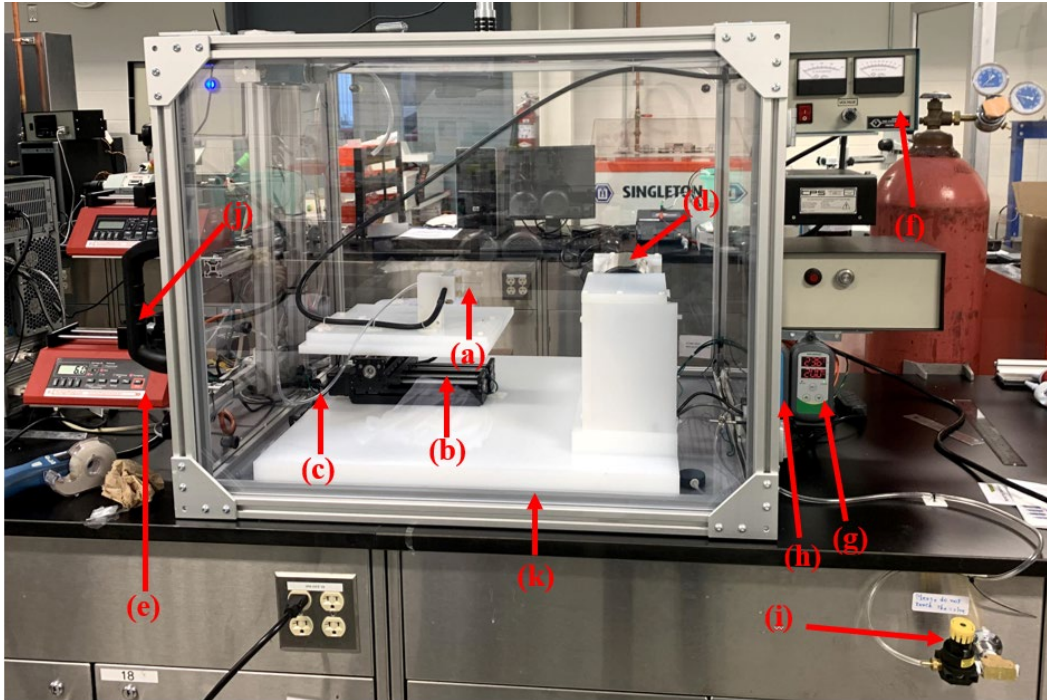


Figure 3. 1 The purpose-built setup for electrospinning instrument in the lab: (a)Needle (b)movement controller (c)solution tube (d)cylinder shaped sample collector (e)syringe driver pump (f)high voltage DC power supply (g)humidity controller (h)temperature controller(i)air valve (j)door handle (k)enclosed glass chamber

The equipment includes the following main components:

(a) Metallic syringe needle delivers an electrical charge to the polymer solution to perform the electrospinning process. A 21-gauge (0.55 mm diameter) stainless steel blunt needle was used. Finer needle diameters present problems with electrospinning of a more viscous solution.

(b) Computer-controlled system to adjust the distance between the syringe needle and the collector. This distance is typically in the range of 10-20 cm.

(c) A 3.175 mm diameter Tigon (polyvinylidene fluoride) flexible tube that transfers the polymer solution to the syringe needle.

(d) Cylindrical rotating drum collector that was electrically connected to ground. The rotation speed was typically 100 rpm, but this could be adjusted up to 1000rpm.

(e) Programmable syringe pump (NE-1002X) that provides a controlled flow rate of the polymer solution to the syringe needle. Flow rates were typically 5 to 20 $\mu\text{L}/\text{min}$.

(f) High voltage DC power supply (Gamma High Voltage Research: ES50P) to charge the polymers solution. Voltages in the range of 10-25 kV are used.

(g) Humidity controller controls the humidity inside the chamber with $\pm 1\%$ accuracy.

(h) Temperature monitor for the inside temperature of the chamber.

3.2 Experimental Details for the Exploratory Study

3.2.1 Materials (PEO and Solvents) used

Poly (ethylene oxide) was purchased from Sigma-Aldrich. The molecular weights range from 100,000 to 5,000,000 g/mol. Full details, including form/color, particle size, purity, assay, and viscosity, are given in Table 3.1. Deionized water (type I) and ethanol were used as a solvent. Full details of solvents are given in Table 3.2.

Table 3. 1 Various molecular weight of PEO

Mv Average#	Form/Color	Particle size	Purity	Assay*	Viscosity (cps)
5,000,000	Powder/White	N/A	N/A	N/A	5500-7500 (1% in H ₂ O at 25°C)
900,000	Powder/White	100% 10 mesh >96% 20 mesh	0.8-3.0% SiO ₂	<1.0%	8800-17,600 (5% in H ₂ O)
600,000	Powder/White	N/A	N/A	N/A	4500-8800 (5% in H ₂ O)
100,000	Powder/White To Off-White	100% 10 mesh 96-100% 20 mesh	N/A	<1.0%	12-50 (5% in H ₂ O)

Mv: Average Molecular Weight

*Assay: Alkalies and other metals (as CaO)

Table 3. 2 Solvents used in the study

Solvent	Details	Supplier
Water	Deionized Ultra-pure Type 1 Resistivity: 18 megaohm.cm	Sigma-Aldrich
Ethanol	95% purity	Greenfield Global

3.2.2 Preparation of Solutions for Electrospinning

Electrospun poly (ethylene oxide) (PEO) fibers were synthesized by first dissolving PEO powder in deionized water (type I) or deionized water/ethanol mixture. Solutions with concentrations varying from 0.5 to 30wt% PEO were made. The solution was stirred overnight at room temperature using a magnetic stirring plate to ensure a homogenous solution. The solution was then poured into a 10 mL syringe attached to a 21-gauge stainless steel needle via a standard polyvinylidene fluoride (PVDF) tubing. The syringe was then inserted into a programmable syringe pump.

3.2.3 Operating Procedures for Electrospinning

Following loading of the solution in the syringe and placement in the syringe pump, a suitable pumping speed was set, ranging between 4.16 to 16.67 $\mu\text{L}/\text{min}$. The rotating cylinder was then placed 10-20 cm from the end of the syringe. High voltage DC power was delivered to the syringe and gradually increased until a stable jet was attained. After every experiment, the high voltage power supply was turned off, and a new layer of aluminum foil was laid on the rotating cylinder. The power was turned on, and samples were collected for 20 minutes for each experiment. Each solution was tested under ambient conditions. To ensure similar conditions, the glass-enclosed chamber temperature and humidity levels were noted for each experiment, and the ambient temperatures were within (20 ± 5) $^{\circ}\text{C}$ and relative humidity levels were within (30 ± 1) % of each process run. Each sample was appropriately stored after ensuring adequate drying of the fibers. These procedures are summarized, step-by-step in Table 3.3.

Table 3. 3 Step-by-step procedures for electrospinning

Steps	Procedure
1.	Make sure the voltage generator and the programmable syringe pump are off.
2.	Fill up the syringe with 10 ml of PEO solution.
3.	Attach the syringe to the polyvinylidene fluoride (PVDF) tube.
4.	Wait for all air bubbles to dissipate from the solution.
5.	Place the syringe in the programmable syringe pump.
6.	Set the desired flow rate in $\mu\text{L}/\text{min}$.
7.	With the help of the motion controller, the distance between the needle tip to the collector is adjusted.
8.	Make sure the voltage supply wire is connected to the needle of the syringe.
9.	Set up the aluminum foil on the rotating collector.
10.	Align the needle in such a manner that it is in the center of the collector.
11.	Turn on the voltage generator.
12.	Adjust the voltage as required for the experiment.
13.	Change the flow rate to the desire flow rate.
14.	Re-adjust the voltage if it is necessary.
15.	If the pendant drop dries out at the needle tip, turn off the voltage generator before cleaning the capillary tip.
16.	Post an electrical hazard sign when the device is running unsupervised.
17.	Use a respirator if the solvent is toxic.
18.	After collecting enough fibers, zero the voltage indicator, then turn off the voltage generator.
19.	Discard the polyvinylidene fluoride (PVDF) tube and clean the valve and collector properly.

3.2.4 Preparation and Characterization of Electrospun Product

3.2.4.1 Optical Microscopy

Optical (light) microscopy has various advantages: the sample preparation is easy, and the instrumentation is comparatively inexpensive. The imaging happens under atmospheric pressure, and the samples do not need to be dried. Consequently, the polymer samples can be examined even when they are wet. Along with the digitization of the signal, optical microscopy allows the checking of the progressions of polymer sample structures during the drying process. Unfortunately, the limiting resolution of optical microscopy is around 200 nm, which prevents the detailed characterization of nanomaterials. An Olympus GX51 optical microscope was used for the preliminary examination of the electrospun product.

3.2.4.2 Scanning electron microscopy (ESEM)

The scanning electron microscope (SEM) is an essential tool capable of producing high-resolution images of a sample surface. SEM measurements were conducted on a field emission scanning electron microscope (FEI Quanta 200 FEG Environmental SEM) equipped with an EDAX Octane Plus SDD X-ray detector: Figure 3.2. The SEM can operate in a Low Vacuum for non-conductive samples, reducing the need for conductive coating. However, the resolution is insufficient for examining nanomaterials. The SEM has a resolution of 3 nanometers in a high vacuum mode and can accommodate wet, dirty, non-conductive, and outgassing samples. The EDAX EDS TEAM software has the potential of a wide variety of materials characterization modes, including simple point analysis, line scans, and element mapping (including multifield maps and phase analysis).



Figure 3.2 FEI Quanta 200 FEG Environmental SEM

This microscope generates images of a sample by examining it with a focused beam of electrons. The electrons interact with atoms in the specimen, producing various signals that can be discovered and that comprise data about the sample surface topography and composition. SEM can attain a resolution better than 1 nanometer. Once the samples were dry, the morphology and diameter of the electrospun nanofibers can be observed by using field emission Scanning Electron Microscopy (SEM). Samples were cut from electrospun mats on an aluminum foil and

mounted on metal stubs using double-sided carbon tape. Before observation, the samples were coated with gold using the plasma sputtering (CGSL1100X-SPC16-3, MTI Corporation) to prevent charging in the ESEM electron beam. See Figure 3.3 for a schematic of sample preparation for SEM. Diameters and distribution evaluation of the electrospun nanofibers were analyzed from the SEM images by using Image J analysis software. For each electrospun mat, several fibers were considered from different locations on the sample to calculate the average fiber diameter (AFD). Outcomes are stated as mean \pm standard deviation.

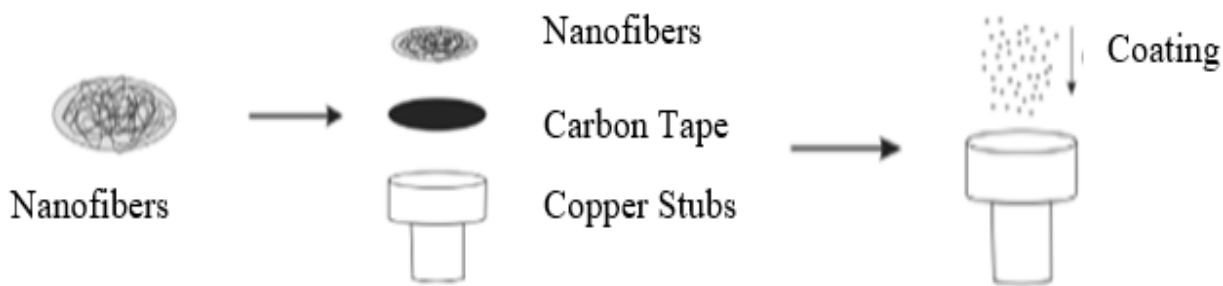


Figure 3. 3 Nanofiber sample preparation for SEM

3.2.4.3 Image J

Various software is available to measure items of the image manually using scale bar calibration. ImageJ software was used for the analysis of the SEM micrographs. ImageJ was developed by the U.S. National Institutes of Health [1, 2]. ImageJ is in the public domain and runs on any operating system. It has found wide usage in many research areas, including nanotechnology [3]. ImageJ is used to determine the diameter of the nanofibers at every pixel along the fiber axis.

3.3 References

1. Rasband, W.S., ImageJ, U.S. National Institutes of Health, Bethesda, Maryland, USA, <https://imagej.nih.gov/ij/>, 1997-2018.
2. Schneider, C.A., Rasband, W.S., Eliceiri, K.W. "NIH Image to ImageJ: 25 years of image analysis". Nature Methods, Vol9, pp. 671-675 (2012).
3. Abramoff, M.D., Magalhaes, P.J., Ram, S.J. "Image processing with ImageJ". Biophotonics International, Vol. 11, No. 7, pp. 36-42 (2004).

CHAPTER 4

RESULTS AND DISCUSSION

This chapter is comprised of a number of sections/sub-sections.

4.1 Summary of Results provides an overview of all experiments conducted during this study, including those from experiments conducted in collaboration with Iman A. Borojeni.

In Section 4.2, an overview is given of the morphology of the electrospun product. This ranges from beads (droplets) to beaded fibers, fibers, and finally to a polymer film, depending on the specific materials/processing parameters.

Sections 4.3 and 4.4 examine the results presented in Section 4.1 in more detail to determine the effects of materials parameters on the product form. Section 4.3 examines the effects of molecular weight/solution concentration on the ability to electrospun PEO nanofibers. This was the major focus of this research study. Section 4.4 examines the effect(s) of the solvent and the advantages/disadvantages of using a water-ethanol mixture as the solvent rather than water only.

Sections 4.5-4.7 examine the effects of processing parameters on the product form. These processing parameters include Voltage (Section 4.5), Needle-to-Collector Distance (Section 4.6), and Flow Rate (Section 4.7). These processing parameters are generally regarded as secondary factors compared to the materials parameters [1, 2]. Examination and discussion of the effects of these processing parameters on product form are, therefore, mainly confined to where they can be compared for a specific set of materials parameters.

Chapter 4 concludes with a discussion of how the morphology of the electrospun product depends on two properties of the PEO solutions, namely intrinsic viscosity (Section 4.8) and entanglement number (Section 4.9).

4.1 Summary of Results

Tables 4.1 – 4.4 provide an overview of all the experiments conducted in this research, including those studies that were conducted in collaboration with Iman A. Borojeni.

Table 4. 1 presents the data for PEO with a molecular weight of 100,000 g/mol

POLYMER	MOLECULAR WEIGHT (g/mol)	SOLVENT	SOLUTION CONCENTRATION(%)	APPLIED VOLTAGE (kV)	RPM	COLLECTION DISTANCE (cm)	FLOW RATE (μL/min)	RESULT		
PEO	100.000	Deionised Water	18	10	500	10	9.16	Few beads and branchy nanofiber structure		
				10		10	14.16	Few beads and branchy nanofiber structure		
				10		15	9.16	Few beads and branchy nanofiber structure		
				10		15	4.16	Few beads and branchy nanofiber structure		
				20		20	9.16	Lots of beads and branchy nanofiber structure		
				15		15	9.16	Lots of beads and branchy nanofiber structure		
				10	40	10	9.17	Lots of beads and branchy nanofiber structure		
				10	40	15	10	Branchy nanofibers turning to film formation due to over-deposition		
				15	20	20	10.83	Few beads and branchy nanofiber structure		
				15	30	10	9.17	Few beads and branchy nanofiber structure		
				20	30	15	10	Few beads and branchy nanofiber structure		
				20	20	20	10.83	Dense web like structure nanofibers with lots of beads		
			20	35	10	9.17	Dense web like structure nanofibers with lots of beads			
			20	30	15	10	Dense web like structure nanofibers with lots of beads			
			20	20	20	10.83	Lots of beads and branchy nanofiber structure			
			20	30	10	9.17	Dense fine nanofibers with few beads and black shadow like patches on the nanofibers			
			22	22	10	10	30	15	10	Nanofibers with very few beads
			10			30	20	10.83	Dense nanofibers with lots of beads and few black shadow like patches on the nanofibers	
			15			30	10	9.17	Lots of beads and branchy nanofiber structure	
			15			30	15	10	Lots of beads and branchy nanofiber structure	
			20			20	20	10.83	Dense web like structure nanofibers with lots of beads	
			20			35	10	9.17	Dense web like structure nanofibers with lots of beads	
			20		30	15	10	Big beads and web like structure turning to almost film formation		
			20		20	20	10.83	Big beads and web like structure turning to almost film formation		
		20	30		10	9.17	Dense fine nanofibers with lots of beads			
		20	30		15	10	Dense web like structure nanofibers with lots of beads			
		20	30		20	10.83	Dense fine nanofibers with lots of beads			
		20	30		10	9.17	Dense fine nanofibers with few beads			
		20	30	15	10	Big beads and web like structure turning to almost film formation				
		20	20	20	10.83	Big beads and web like structure turning to almost film formation				
		20	35	10	9.17	Few beads and branchy nanofiber structure				
		20	30	15	10	Few beads and branchy nanofiber structure				
		20	20	20	10.83	Few beads and branchy nanofiber structure				
		20	15	10	6	Dense web like structure nanofibers with few beads				
		20	20	10	16.67	Dense web like structure nanofibers with few beads				
		20	20	15	6	Dense branchy nanofibers with few beads				
		20	25	15	16.67	Dense web like structure nanofibers with few beads turning to film formation				
		20	20	20	6	Dense branchy nanofibers with few beads				
		20	25	20	16.67	Dense branchy nanofibers with few beads				
		20	15	100	10	6	Defect-free dense fine web like structure nanofibers			
		20	15	100	10	16.67	Defect-free dense fine nanofibers			
		20	15	100	15	6	Defect-free dense fine nanofibers			
		20	15	100	15	16.67	Defect-free dense fine nanofibers			
		20	15	110	20	6	Defect-free dense fine nanofibers			
		20	15	110	20	16.67	Defect-free dense web like structure nanofibers			
		20	20	10	6	Big beads and web like structure turning to almost film formation				
		20	20	10	16.67	Big beads and web like structure turning to almost film formation				
		20	25	15	6	Lots of big beads and branchy nanofiber structure				
20	25	15	16.67	Lots of big beads and branchy nanofiber structure						
20	20	20	6	Lots of big beads and branchy nanofiber structure						
20	25	20	16.67	Lots of big beads and branchy nanofiber structure						
22	22	Deionised Water	10	100	10	6	Defect-free web like structure nanofibers			
15			100	10	16.67	Defect-free web like structure nanofibers turning to almost film formation				
10			100	15	6	Defect-free dense fine nanofibers				
15		100	15	16.67	Defect-free dense fine nanofibers					
20		110	20	6	Defect-free dense fine nanofibers					
20		110	20	16.67	Defect-free dense fine nanofibers					
20	Deionised Water-Ethanol	Deionised Water	10	100	10	6	Defect-free web like structure nanofibers			
15			100	10	16.67	Defect-free web like structure nanofibers turning to almost film formation				
10			100	15	6	Defect-free dense fine nanofibers				
15		100	15	16.67	Defect-free dense fine nanofibers					
20		110	20	6	Defect-free dense fine nanofibers					
20		110	20	16.67	Defect-free dense fine nanofibers					

Table 4. 2 presents the data for PEO with a molecular weight of 600,000 g/mol

POLYMER	MOLECULAR WEIGHT (g/mol)	SOLVENT	SOLUTION CONCENTRATION(%)	APPLIED VOLTAGE(kV)	RPM	COLLECTION DISTANCE (cm)	FLOW RATE (μL/min)	RESULTS
PEO	600,000	Deionised Water	4.5	15	500	15	9.16	Dense defect-free fine nanofibers
				15		15	14.16	Dense defect-free fine nanofibers
				20		20	9.16	Dense defect-free fine nanofibers
				20		20	14.16	Dense defect-free fine nanofibers
				10		10	9.16	Film like structure with few tiny beads and couple of nanofibers
				10		10	14.16	Just two fine nanofibers on the entire sample
				15		10	9.16	Few defect-free fine nanofibers
			5	10	1024	10	6	Defect-free fine nanofibers
				10		10	16.67	Dark shadows on defect-free nanofibers due to over-wetting
				10		15	16.67	Dense defect-free fine nanofibers
				10		15	16.67	Dense defect-free fine nanofibers
				15		20	6	Dense defect-free fine nanofibers
				15		20	16.67	Dense defect-free fine nanofibers
				15		10	100	10
		15	15	6	Fibers			
		15	10	16.67	Film			
		15	15	16.67	Fibers, a lot of circular defects			
		Deionised Water-Ethanol	5	100	20	16.67	Fibers, few circular defects	
					15	10	6	Film
					15	15	6	Film
					15	20	6	Fibers
					15	10	16.67	Film
					15	15	16.67	Film
					15	20	16.67	Film
			2.5	7	100	10	6	Fibers and merged structure
				7		15	6	Fibers with a few beads
				8		20	6	Fibers with a few beads
				9		10	16.67	Film
10	15			16.67		Fibers with a few beads and merged structure		
10	20			16.67		Fibers with a few beads		
12	20			16.67		Fibers with a few beads		

Table 4. 3 Presents the data for PEO with a molecular weight of 900,000 g/mol

POLYMER	MOLECULAR WEIGHT (g/mol)	SOLVENT	SOLUTION CONCENTRATION(%)	APPLIED VOLTAGE(kV)	RPM	COLLECTION DISTANCE (cm)	FLOW RATE (μL/min)	RESULTS
PEO	900,000	Deionised Water	2	10	100	10	6	Beads
						15		Beads
						20		Beads
			10	16.67		Film, beads		
			15			Beads		
			20			Beads		
		10	6	Film				
		15		Fibers				
		20		Fibers				
		10	16.67	Film				
		15		Fibers with wide size range distribution and merged structure, a lot of circular defects				
		20		Fibers, few circular defects				
	Deionised Water-Ethanol	2	8	100	20	6	Fibers with beads, circular defects	
					10	16.67	Fibers with beads, circular defects	
					20	16.67	Fibers with beads, circular defects	
		3	7		6	Film		
			8			Fibers, few circular defects		
			10			Film		
		10	16.67	Film				
		10		Film				
		15		Film				
		4	10	6	Film			
			10		Film			
			10		Film			
10	16.67		Film					
10			Film					
10			Film					

Table 4. 4 presents the data for PEO with a molecular weight of 5,000,000 g/mol

POLYMER	MOLECULAR WEIGHT (g/mol)	SOLVENT	SOLUTION CONCENTRATION(%)	APPLIED VOLTAGE(kv)	RPM	COLLECTION DISTANCE (cm)	FLOW RATE (μL/min)	RESULTS
PEO	5,000,000	Deionised Water	0.5	15	100	20	6	Few semi fibers, film
		Deionised Water-Ethanol		10		20	6	Film
		Deionised Water-Ethanol	0.6	15	500	15	9.16	Beaded fibers
				15		15	14.16	film
				20		20	9.16	film
				20		20	14.16	film
				10		10	9.16	Beaded fibers
				10		10	14.16	Beaded fibers
				15		10	9.16	Beaded fibers
				10		10	6	Beaded fibers
		Deionised Water	0.6	10	1024	10	16.67	Beaded fibers
				10		15	16.67	Beaded fibers
				10		15	16.67	Beaded fibers
				15		20	6	Beaded fibers
				15		20	16.67	Beaded fibers
				10		10	4.16	Few semi fibers, film
				10		10	6	Few semi fibers, film
				15		10	9.16	Few semi fibers, film
		Deionised Water	1	20	100	10	16.67	Beaded fibers, film
				10		15	4.16	Few semi fibers, film
				10		15	6	Few semi fibers, film
				15		15	9.16	Few semi fibers, film
				20		15	16.67	Beaded fibers , film
10	20			4.16		Few semi fibers, film		
10	20			6		Few semi fibers, film		
10	20			6		Few semi fibers, film		
Deionised Water	1	10	100	20	6	Few semi fibers, film		
Deionised Water-Ethanol		15		20	6	Few semi fibers, film		

Included in these tables are details of the material parameters (molecular weight of PEO, solvent, solution concentration) and processing parameters (applied voltage, rotation speed of collector, needle-to-collector distance, and flow rate) together with a short description of the electrospun product. As noted in Chapter 3, the temperature was controlled at $23\pm 3^{\circ}\text{C}$, and the relative humidity was controlled at $30\pm 1\%$.

Solution concentrations investigated varied from 30% to 0.5%: a higher concentration was used for the lower molecular weight PEO. The applied voltage was varied from 7-25 kV, with most electrospinning runs being conducted at an applied voltage of 10, 15, or 20 kV. For most tests, the collector rotation speed was set at 100 rpm, although lower and higher speeds were examined to determine the effects of rotation speed. The needle-to-collector distance was varied from 10 to 20 cm. Flow rates were varied from 4.16 to 16.67 $\mu\text{L}/\text{min}$.

Table 4.1 presents the data for PEO with a molecular weight of 100,000 g/mol. Table 4.2 is for 600,000 g/mol. Table 4.3 is for 900,000 g/mol. Table 4.4 is for 5,000,000 g/mol. In Tables 4.2, 4.3, and 4.4, results from the collaborative study with Iman Borojeni are indicated in red text.

4.2 Morphology of Electrospun Nanofibers

Any soluble polymer with appropriately high molecular weight can be electrospun. Nanofibers made of natural polymers, polymer blends, nanoparticle or drug-impregnated polymers, and ceramic precursors can also be successfully electrospun. Various fiber morphologies have also been demonstrated in Figure 4.1, such as beaded, branchy, web-like, defect-free, over-wetting of web-like structure, and film.

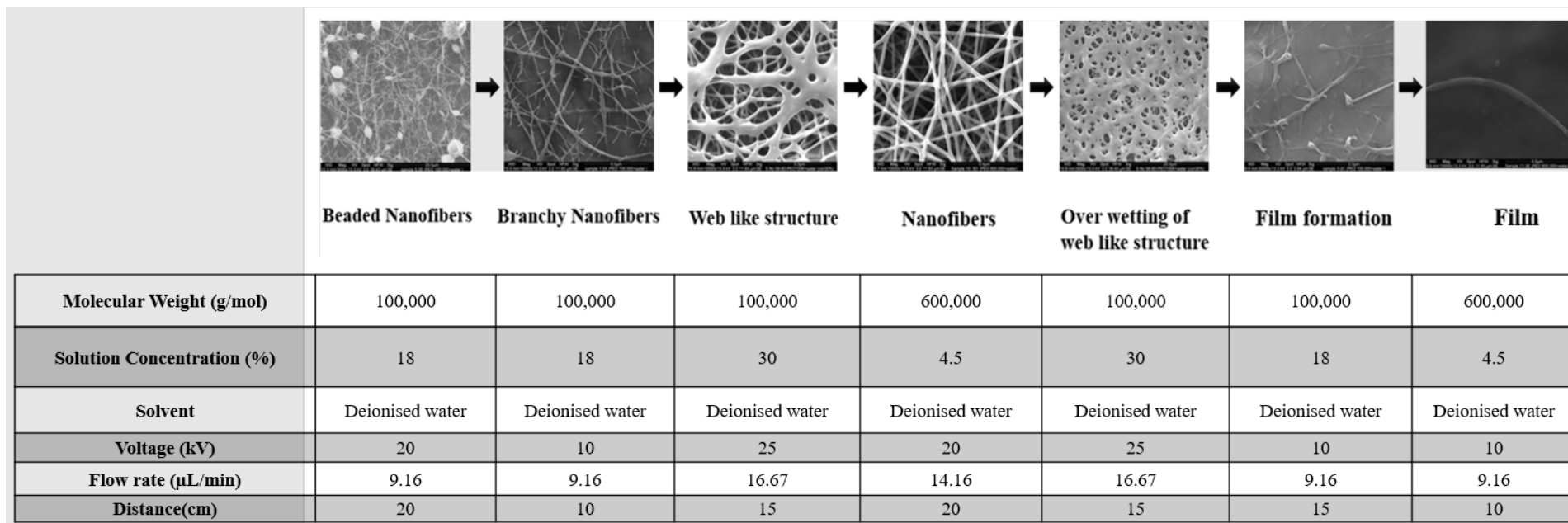


Figure 4.1 Range of products

4.3 Effect of Molecular Weight & Solution Concentration on the morphology of nanofibers

The solution concentration performs a substantial role in stabilizing the fibrous structure. Several polyethylene oxide polymers of various molecular weights were obtained. Mark (1938) [3] and Houwink (1940) [4] independently correlated the intrinsic viscosity with molecular weight for various polymers.

$$[\eta] = kM^a \quad \text{Equation 4.1}$$

Where k and a both are Mark-Houwink constants and $[\eta]$ is intrinsic viscosity in ml/g. For PEO in water, k is 1.25×10^{-2} (0.0001250) and a is 0.7800 [5].

PEO's molecular weight and the solution concentration have a significant effect on the structure of the electrospun polymer. At each Mw, there is a minimum concentration (C) needed to stabilize the fibrous structure and maximum concentration where the solution cannot be electrospun. Fibrous structures were generally obtained at $[\eta]C > 1$ (Figure 4.2- B & C). The fibers contained many branches, web-like structures, or irregular diameter fibers and were highly interconnected. Typical fiber diameters were between 100 nm and 2 μm . The fiber diameter increases with Mw. At low concentrations of higher Mw ($[\eta]C < 21$) see Figure 4.2- B, C, & D mostly fine defect-free fibers were obtained. As the solution concentration increases, the fiber diameter, and interfiber spacing increase, and there is a gradual shift from branchy to web-like structure fibers. In low molecular weight samples, this shift from branchy to web-like structure fibers occurs at a higher value of concentration than in polymers with high Mw. Film formations are typically observed when $[\eta]C > 21$ (Figure 4.2- A). Structures obtained at equal values of $[\eta]C$ are generally similar at low to moderate Mw values. However, at high Mw, a broad distribution of fibers, with a significant number of large fibers, is observed for the same value of $[\eta]C$.

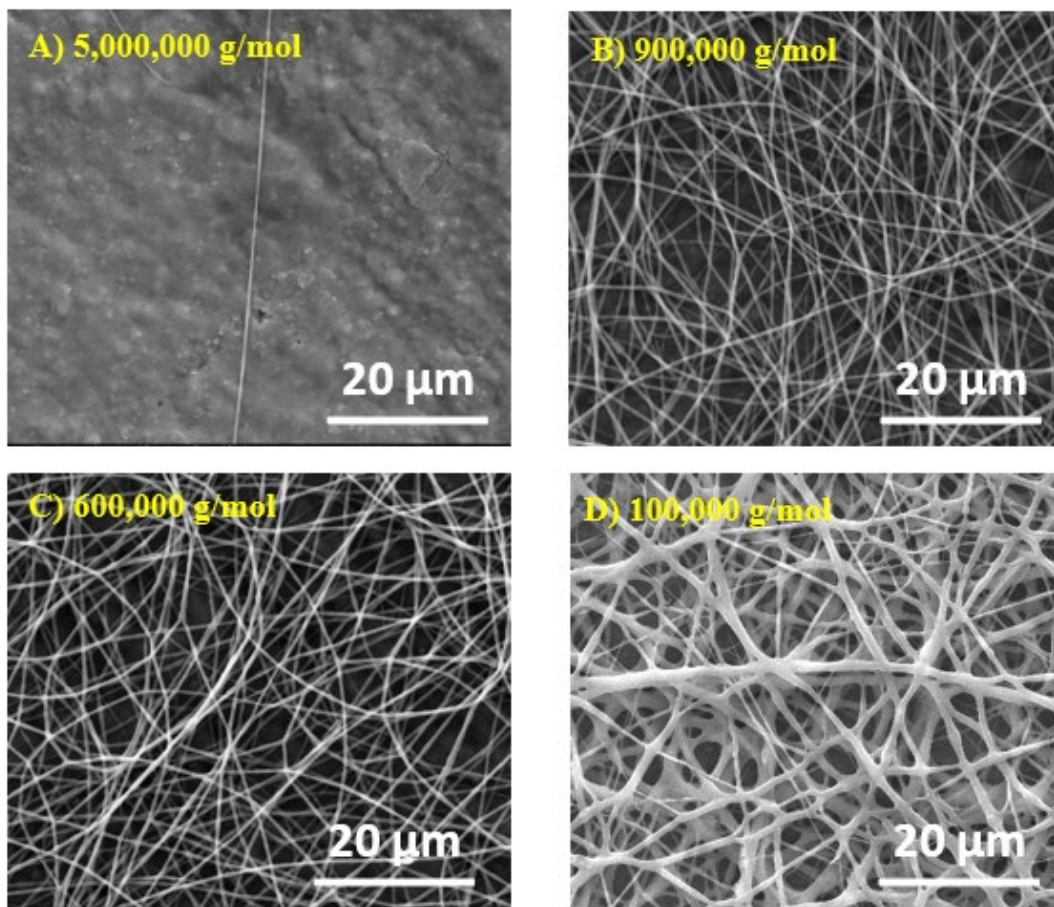


Figure 4.2 The SEM micrographs of the electrospun fibers from the different molecular weights of PEO water solution when flow rate (F) = 6 $\mu\text{L}/\text{min}$ and working distance (D) = 20 cm

From the SEM micrographs of 900,000 g/mol PEO in water-ethanol solution, Solution concentration had a significant impact on the morphology of the nanofibers. The morphology images are shown in Figure 4.3 (A-C).

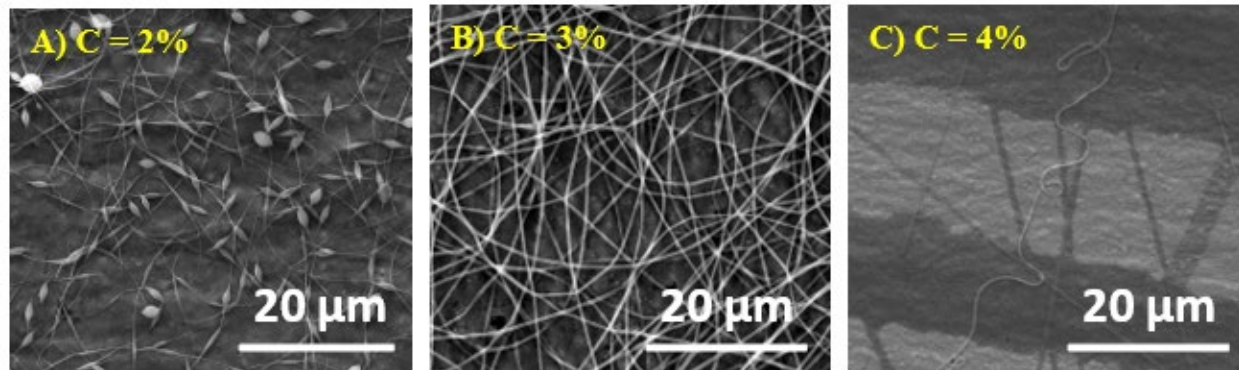


Figure 4.3 The SEM micrographs (SE) of the electrospun deposition (beaded fibers, fibers, and film) from different concentrations(C) of PEO (900 KDa) in water-ethanol solution when the flow rate = 6 μ L/min and working distance = 20cm

The deviation from optimum concentration can have a more profound impact on the quality of the obtained electrospun product. Figure 4.3-A shows the electrospun mats from the water-ethanol solution mixture when the concentration of PEO was 2wt%. The fibers were heavily degraded from bead formation. On the other hand, when the concentration of PEO increased to 4wt%, film formation was promoted due to extremely low bending instabilities even when a long working distance (20cm) and low flow rate (6 μ L/min) was considered (Figure 4.3-C). The polymer solution's viscoelasticity dependency was very sensitive to the concentration when the molecular weight increased to 900,000 g/mol. If the concentration was low (2wt%), the viscoelasticity was not sufficient for making defect-free fibers. In this case, the surface energy became the dominant factor to dictate the fiber's morphology, which led to bead formation (Figure 4.3-A).

On the other hand, when a higher concentration (4wt%) was applied, the polymer solution's viscoelasticity increased drastically, preventing bending instabilities during the electrospinning process. Therefore, the jet did not dry entirely when it reached the collector, the mat became over-wet, and film formation took place (Figure 4.3-C). Applying a medium concentration (3wt%) was an effective strategy to obtain defect-free fibers (Figure 4.3-B). However, producing a defect-free mat from a medium concentration solution was sensitive to the processing conditions. Only when the flow rate was low (6 μ L/min) and the working distance was between 15 to 20 cm, were fibers produced, and films were formed in other cases. Therefore, for successful electrospinning of

900,000 g/mol from ethanol-water mixture solution, both solution, and processing conditions should be tuned carefully.

Bead formation started at lower solution concentrations, and the increase in fiber diameter with an increase in solution concentration is attributed to the changes in the solution's viscosity. Solution viscosity is correlated to the extent of polymer chain molecules entanglement within a solution [6]. An increase in polymer chain entanglement due to the increase in the number of polymer molecules increases its viscosity [7]. During electrospinning, a low viscosity solution possesses a low viscoelastic force, which cannot match the electrostatic and columbic repulsion forces that stretch the electrospinning jet. This causes the jet to break up partially [8]. Under the effect of surface tension, the high numbers of free solvent molecules in the solution come together into a spherical shape causing the formation of beads [9, 10]. When solution concentration is increased, viscosity increases, causing an improvement in the viscoelastic force. Hence, the partial breakup of the jet is prevented. The increased polymer chain entanglement with an increase in solution concentration also enables the solvent molecules to be distributed over the entangled polymer molecules, leading to smooth fibers' formation and improved fiber uniformity [11,8] as shown schematically in Figure 4.4 (a-d).

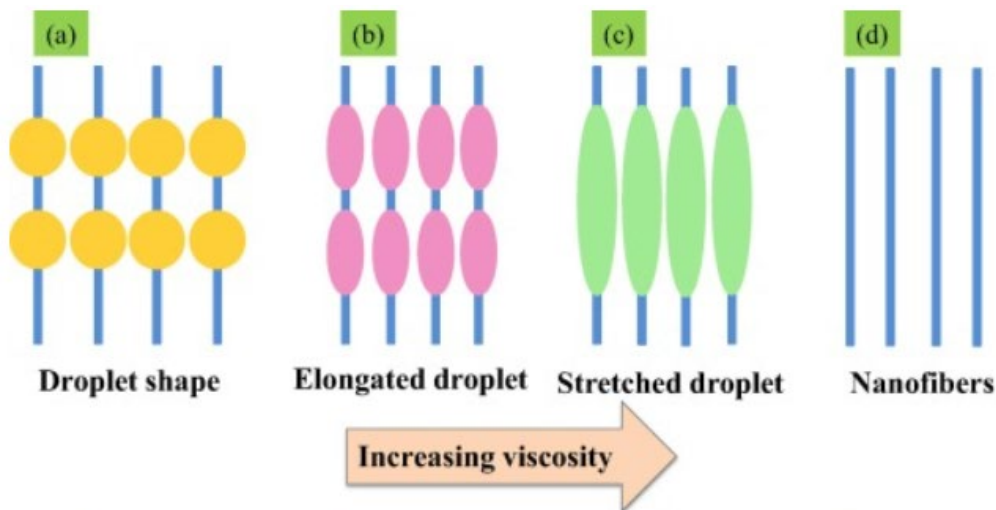


Figure 4.4 Variation in morphology of electrospun nanofibers of PEO with viscosity: (a–d) [12]

4.4 Effect of Solvent on the morphology of nanofibers

The flexibility of the electrospinning procedure allows to effortlessly engineer fiber morphology to desired specifications before, by adjusting various parameters that control the spinning process. The selection of the solvent is one of the key factors for the formation of smooth and defect-free electrospun nanofiber. Generally, two factors need to be kept in mind prior to pick the solvent. First, the preferred solvents for electrospinning process have polymers that are completely soluble. Second, the solvent should have a moderate boiling point. Its boiling point gives an idea about the volatility of a solvent. The use of two solvents with different boiling points to spin the same polymer is included.

SEM images are presented for poly (ethylene oxide) PEO spun with deionised water (Figure 4.5-A) and deionised water- ethanol (Figure 4.5-B) keeping all other parameters constant. The use of a lower boiling point solvent can drastically modify the fiber morphology by increasing fiber diameter due to the fast evaporation of alcohol during the spinning process as shown in Figure 4.5-B. This not only affects the sample morphology, but it also affects the mechanical properties. However, highly volatile solvents are mostly avoided because their low boiling points and high evaporation rates cause the drying of the jet at the needle tip. Constantly drying will block the needle tip, and hence will obstruct the electrospinning process. Similarly, less volatile solvents are also avoided because their high boiling points prevent their drying during the nanofiber jet flight. The deposition of solvent-containing nanofibers on the collector will cause the formation of beaded nanofibers as shown in Figure 4.5-A.

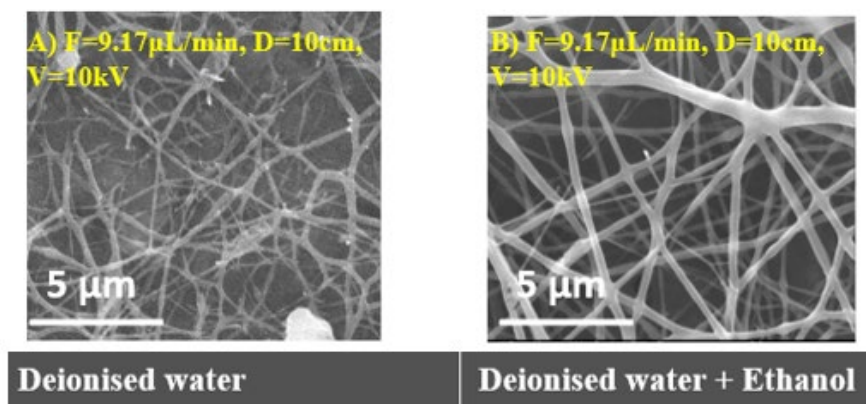


Figure 4.5 The SEM micrographs of the electrospun fibers from 100 KDa PEO with concentration 18 % under different solvents and constant voltage (kV), the working distance (D), flow rate (F)

4.5 Effect of Voltage on the morphology of nanofibers

Generally, it is a known fact that the flow of current from a high-voltage power supply into a solution *via* a metallic needle will cause a spherical droplet to deform into a Taylor cone and form ultrafine nanofibers at a critical voltage [13]. The critical value of applied voltage fluctuates from polymer to polymer. Several variables can manipulate the electrospinning process. These can be categorized as materials, processing, and environmental parameters. The electric field strength during the electrospinning process depends on the applied voltage which may affect electrospun fibers' morphology.

Applied voltage provides the surface charge on the electrospinning jet. Therefore, the jet's instability and stretching increase with applied voltage, generally leading to smaller fiber diameters as shown in Figures 4.6 A, B, & C. As the voltage increases, the jet becomes unstable, which results in fine fibers, as shown in Figure 4.6- C. It is not necessary that with the lower voltage, the jet is stable. However, it can also result in stable and discontinuous jet flow (Figure 4.6- A shows many broken fine nanofibers). The formation of smaller-diameter nanofibers with an increase in the applied voltage is attributed to the polymer solution's stretching in correlation with the charge repulsion within the polymer jet [14]. An increase in the applied voltage beyond the critical value will result in beads or beaded nanofibers. The increases in the diameter and formation of beads or beaded nanofibers with an increase in the applied voltage are attributed to the decrease in the Taylor cone's size and increase in the jet velocity for the same flow rate (Figure 4.6- B shows small nodes in fibers). Furthermore, the diameter of the nanofibers was also increased with an increase in the applied voltage.

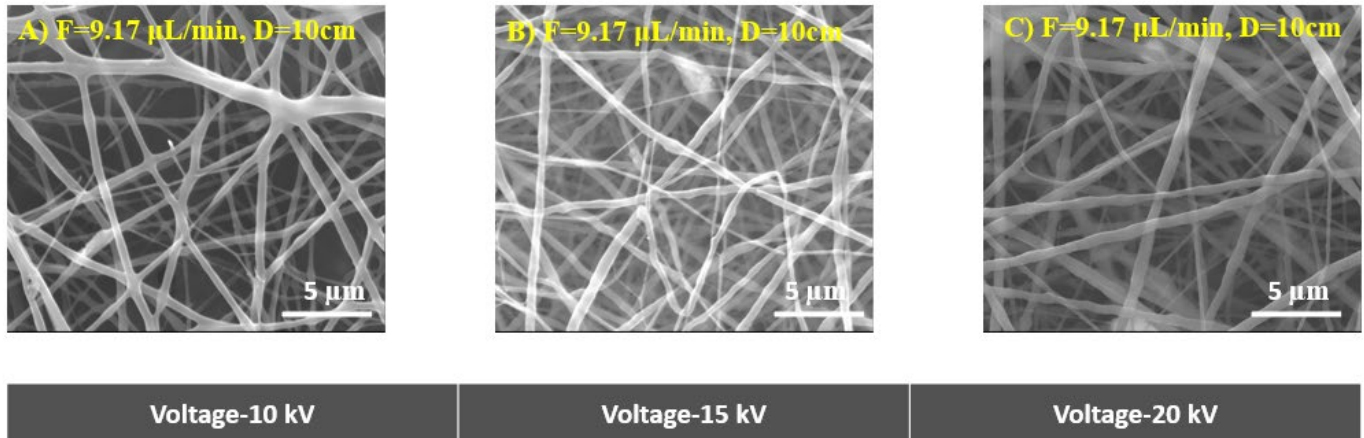


Figure 4.6 The SEM micrographs of the electrospun fibers from 100 KDa PEO water-ethanol solution with concentration 18 % under different voltages (kV), the constant working distance (D), and flow rate (F)

4.6 Effect of Distance from needle tip to the collector on the morphology of nanofibers

The distance between the metallic needle tip and collector plays an essential role in determining an electrospun nanofiber's morphology. Similar to the applied electric field, viscosity, and flow rate, the distance between the metallic needle tip and collector also varies with the polymer system. The nanofiber morphology could be easily affected by the distance because it depends on the deposition time, evaporation rate, and whipping or instability interval [15]. Figure 4.7 A & D shows that when the distance between the needle and the collector is too close, which is 10 cm, it does not give enough time to evaporate the polymer solution. As a result, it ends with over wetting, beaded fibers, or defective fibers. Increasing the distance beyond the critical value not only leads to fine fiber formation but also defect-free fibers formation due to complete drying of the nanofiber jet during the flight between the needle tip and the collector distance see Figure 4.7 B, C, E, & F.

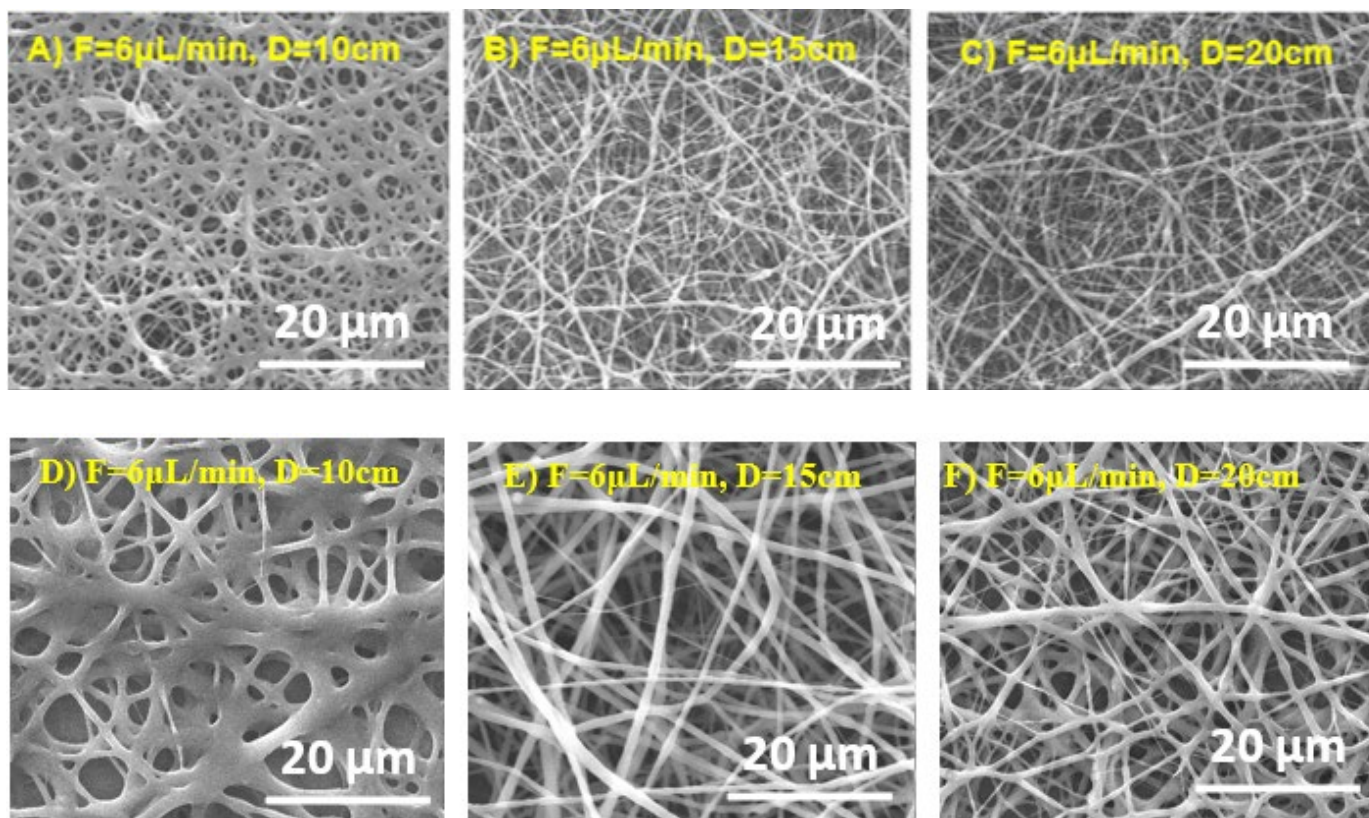


Figure 4.7 The SEM micrographs of the electrospun fibers from 100 KDa PEO water-ethanol solution with concentration 30 % under different working distances (D) and constant flow rates (F)

Hence, a critical distance needs to be maintained to prepare smooth and uniform electrospun nanofibers. Any changes on either side of the critical distance will affect the nanofibers' morphology [16]. The distance between the needle tip and collector and concluded that defective and large-diameter nanofibers are formed when this distance is kept small, whereas the diameter of the nanofiber decreased as the distance was increased [15,17,18].

4.7 Effect of Flow Rate on the morphology of nanofibers

The flow of the polymeric solution through the metallic needle tip determines the morphology of the electrospun nanofibers. Uniform defect-free electrospun nanofibers could be prepared *via* a critical flow rate for a polymeric solution. The critical value fluctuates with the polymer system. Increasing the flow rate above the critical value might lead to bead formation. For instance, in poly (ethylene oxide) PEO, when the flow rate was increased to 16.67 $\mu\text{L}/\text{min}$, over wetting fiber

formation was observed. However, when the flow rate was reduced to 6.00 $\mu\text{L}/\text{min}$, bead-free nanofibers were formed. Increasing the flow rate beyond a critical value leads to increased pore size and fiber diameter to bead formation or over-wetting fibers formation (due to incomplete drying of the nanofiber jet during the flight between the needle tip and metallic collector) [19].

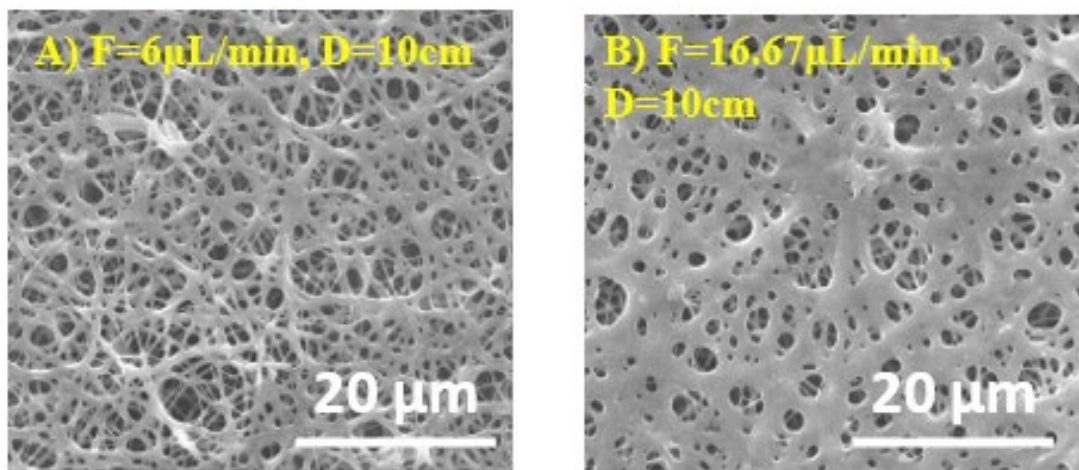


Figure 4.8 The SEM micrographs of the electrospun fibers from 100 KDa PEO water solution with concentration 30 % under different flow rates (F) and a constant working distance (D)

Since increases and decreases in the flow rate influence the nanofiber structure formation and diameter, a minimum flow rate is chosen to retain a balance between the departing polymeric solution and replacing that solution with a new one during jet formation [19, 20]. This will also allow forming a stable jet cone and sometimes a receded jet (a jet that emerges directly from the inside of the needle with no apparent droplet or cone). Receded jets are not stable jets, and during the electrospinning process, these jets are continuously replaced by cone jets. As a result of this phenomenon, nanofibers with a wide range diameter are formed (Figure 4.8-A) [12]. In addition to bead formation, in some cases, at an elevated flow rate, ribbon-like defects [19] and web-like structure turning to film formation begin (Figure 4.8-B). The formation of beads and ribbon-like structures with an increased flow rate was mainly attributed to the solvent's non-evaporation and inadequate stretching of the solution in the flight between the needle and metallic collector. The same effect could also be attributed to an increase in the nanofiber's diameter with an increase in the flow rate, as shown in Figure 4.8-B. The presence of the unspun droplets is attributed to the gravitational force's influence [12]. Another important factor that may cause defects in the nanofiber structure is the surface charge density. Any variation in the surface charge density may

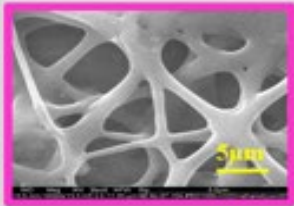
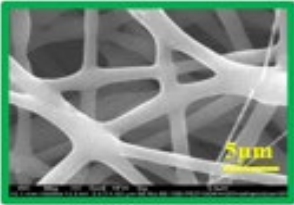
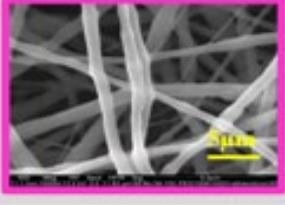
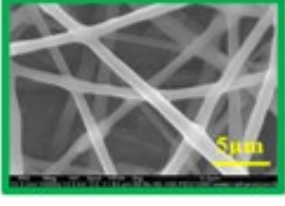
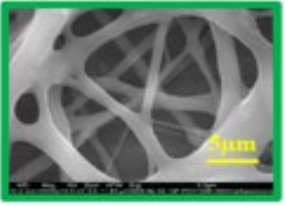
also change the morphology of the nanofiber. For instance, Theron et al. [22] revealed that the flow rate and electric current are directly related. Theron et al. [22] studied the effects of the flow rate and surface charge density using various polymers, including PEO, polyacrylic acid (PAA), polyvinyl alcohol (PVA), polyurethane (PU), and polycaprolactone (PCL). They observed an increase in the flow rate simultaneously increased the electric current and decreased surface charge density. A reduction in the surface charge density will allow the merging of electrospun nanofibers during their flight toward the collector. This merging of nanofibers facilitates garland formation [21, 22].

4.8 Image J analysis of fiber diameter

The image analysis was confined to the samples for 100,000 g/mol. PEO in a water-ethanol solvent. The applied voltage was kept constant at 15 kV, and the rotation speed of the collector drum was 100 rpm. Collection distances were 10, 15, or 20 cm and flow rates were 6 or 16.67 $\mu\text{L}/\text{min}$.

Table 4.5 summarizes the effect of collector distance and flow rate on the average, maximum, and minimum diameters. The first point to note is the wide range of diameters (maximum to minimum) for each combination of processing parameters. Secondly, varying the collector distance between 10 to 20 cm and the flow rate from 6 to 16.67 $\mu\text{L}/\text{min}$ had little or no effect on the average fiber diameter. Within this set of material/processing parameters, fibers were always produced.

Table 4. 5 The effect of collector distance and flow rate on the average, maximum, and minimum diameters (\pm standard deviation from Image J software)

Collector Distance (cm)	Average Diameter (nm)	Maximum Diameter (nm)	Minimum Diameter (nm)	SEM Micrographs
10	545 \pm 22.36	1007 \pm 22.36	269 \pm 22.36	
	536 \pm 16.43	1100 \pm 16.43	65 \pm 16.43	
15	498 \pm 18.96	985 \pm 18.96	101 \pm 18.96	
	542 \pm 10.05	887 \pm 10.05	279 \pm 10.05	
20	—	—	—	—
	557 \pm 11.62	2348 \pm 11.62	55 \pm 11.62	

(Flow rate: 6 μ L/min, 16.67 μ L/min)

4.9 Effect of Viscosity/*Intrinsic Viscosity on the morphology of nanofibers*

Viscosity is a measure of the resistance to flow when one layer of the fluid moves with another. The viscosity is usually measured in Poise (P) or Centipoise (cP). In the SI system 1 cP = 1 mPa.s.

Intrinsic viscosity $[\eta]$ measures the solute's contribution to a solution's viscosity. It does not have the same units of measure as absolute viscosity, i.e., Poise or Pa·s, but rather the unit of measure is ml/g (a concentration measure). Intrinsic viscosity is determined by measuring the relative viscosity at several different concentrations and then extrapolating the specific viscosity to zero concentration [23].

Table 4.6 summarizes the effect of the molecular weight on the viscosity of PEO-water solutions with 5% PEO. Highlighted in Table 4.6 is the Mw (molecular weights) investigated in this study. Two trends are evident. First, for a fixed concentration of PEO, the viscosity of a PEO-water solution increases with increasing Mw of the PEO. Secondly, for any nominal Mw, the measured values of viscosity vary over a wide range. The variation in viscosity for a nominal molecular weight is discussed in section 2.5.2 (i) of this thesis, due to polydispersity, where the polymer is composed of chain lengths that vary over a range of molecular masses.

Table 4. 6 Viscosity of solutions of PEO of varying molecular weight in water (all 5% solutions unless otherwise indicated)

Molecular weight (g/mol)	Viscosity (cP)
100,000	12-50
200,000	65-15
300,000	600-1200
400,000	2250-4500
600,000	4500-8800
900,000	8800-17,600
2,000,000 (2% in H ₂ O)	2000-4000
5,000,000 (1% in H ₂ O)	5500-7500

The trend of increasing viscosity with increasing molecular weight of the PEO is also seen in data for the intrinsic viscosity, Table 4.7 [24], where the contribution of the solute (PEO) to the viscosity of a solution increases with the molecular weight of the PEO. Table 4.7 contains (in red text) extrapolated values of the intrinsic viscosity for the four molecular weights investigated in this study.

Table 4. 7 Intrinsic viscosity of PEO in water [24]

Molecular weight (Kg/mol)	Intrinsic viscosity (ml/g)
99	88.9
100	~ 90
370	303.5
600	~ 360
900	~ 460
1100	539.1
4600	1290.4
5000	~ 1300
8000	1410

Doshi and Reneker, in their "classic" 1995 paper [25], found that viscosity of 800-4000 cP was required to electrospin PEO as fibers. Examination of Table 4.6 indicates that 5% solutions in the water of PEO with Mw of 300,000 or 400,000 g/mol fit in the viscosity range required to form fibers. A 2% solution in water of the 2,000,000 g/mol PEO should also produce fibers in electrospinning.

Table 4.8 presents our observations of the effect of concentration (%) of PEO on the morphology of the resulting electrospun product.

Table 4. 8 Effect of Molecular weight, Concentration, and Solvent on the electrospun product for PEO

Molecular Weight (g/mol)	Deionised Water	Deionised Water-Ethanol
100,000	18% - 30 % beads → branched → web structure	18% - beads + web structure 22% - nanofibers 30% - nanofibers
600,000	4.5% - nanofibers 5.0% - nanofibers (defect fibers/ film at low rotation speed)	2.5% - beaded nanofibers 5.0% - fibers/film
900,000	2% - beads/film 4% - fibers/film	2% - beaded fibers 3% - fibers/film 4% - film
5,000,000	0.5% - few fibres/film 0.6% - film fibers 1.0 % - film	0.5% - film 0.6% - film 1.0% - film (few fibers)

Again, using the Doshi and Reneker criteria for fiber formation, i.e., a viscosity 800-4000 cP, the examination of Table 4.6 shows that for Mw = 100,000 g/mol, a PEO concentration greater than 5% would be required to raise the viscosity of the solution above the 800 cP lower limit for fiber formation. Table 4.8 shows that >30% PEO is required to form fibers (30% was the highest concentration examined). For Mw 600,000 g/mol, Table 4.6 indicates that a PEO concentration slightly less than 5% would be required for the viscosity to be below Doshi and Reneker's upper limit (4000 cP). Defect-free nanofibers were formed at a PEO concentration of 4.5%. At 5% PEO concentration, defect-free nanofibers were only formed at a high collector rotation speed.

For 900,000 g/mol PEO, Table 4.6 would suggest that a concentration of 5% would produce a viscosity very much higher than Doshi and Reneker's upper limit for fiber formation. As shown in Table 4.8, both 2% and 4% concentration produced a film deposit, typical of a higher viscosity solution. Some beads were formed at 2% concentration and fibers at 4% concentration.

For the 5,000,000 g/mol PEO, Table 4.6 indicates that even a 1% solution would have a viscosity higher than Doshi and Reneker's upper limit. As can be seen in Table 4.8, 1% of PEO produced only a film. For 0.5% and 0.6%, there was film formation, but a few fibers were also formed.

Table 4.8 also shows the product form when the solvent was changed to a water-ethanol mixture. For 100,000 g/mol PEO, nanofibers were formed at both 22% and 30% concentrations. For the 600,000 g/mol PEO and 5% concentration, a film was formed. For the 900,000 g/mol PEO, similar structures were formed in the water-ethanol solvent as for water only, with a film being the major constituent. For the 5,000,000 g/mol PEO, the primary product was a film, although there was some evidence of fewer fibers being formed in the water-ethanol solvent than in the water only solvent. All these observations are consistent with an assumption that the viscosity of the solution is higher for the water-ethanol solvent than for water only.

4.10 Effect of Entanglement Number on morphologies of nanofibers

In a polymer, entanglements develop from the interpenetration of random coil chains. They are considered as a network of bridges, where a bridge is a segment of a polymer chain which is long enough to form one loop on itself: see Figure 4.9 [26].

- Entanglements develop from the interpenetration of random coil chains
- They are considered as a network of bridges, where a bridge is a segment of a polymer chain which is long enough to form one loop on itself



Figure 4.9 Entanglements in polymer melts [26]

Entanglements are essential in controlling the rheology of polymers, both in the melt and in the solution. A log-log plot of melt viscosity vs. M_w , at first shows a slow linear increase in viscosity with M_w . At some point, known as the Critical Entanglement Weight (M_c), a strong sudden onset

of strong viscosity changes with increasing molecular weight. Similar behavior is found for the viscosity and the concentration of a polymer in solution [27]. This change in viscosity, reflecting the increasing number of entanglements, thus affects the nature of the electrospun product [27, 28].

For a given polymer-molecular weight-concentration in solution, an entanglement number ($(n_e)_{\text{soln}}$) is defined as [29]:

$$(n_e)_{\text{soln}} = \frac{\phi M_w}{M_e} \quad \text{Equation 4.2}$$

Where ϕ = Volume fraction of PEO in solution

M_w = Molecular Weight

M_e =Entanglement Molecular Weight

For PEO, $M_e \approx 2000$ [30-32]

M_e for polymer solutions is the equivalent of M_c for polymer melts.

Figures 4. 10 (a) and (b) present a summary of all results obtained for all four molecular weights, both in water and water-ethanol solvents. The table in Figure 4.10 (a) demonstrates the relationship between the entanglement number ($(n_e)_{\text{soln}}$) and the morphology of the electrospun product (color-coded to correspond to a particular morphology). Figure 4.10 (b) are SEM micrographs of the different morphologies produced by electrospinning. The borders of the micrographs are color-coded to correspond to the morphologies given in Figure 4.10 (a). Nanofibers are formed for $(n_e)_{\text{soln}}$ values between 13.5-15. Lower values of $(n_e)_{\text{soln}}$ produce beads or beaded fibers. Higher values of $(n_e)_{\text{soln}}$ produce film structures.

Molecular Weight Mw (g/mol)	Volume fraction ϕ (wt%)	M_w/M_e	$(n_e)_{soln}$	Results
100,000	18	50	9	Beaded Fibers
	22		11	Beads + Branchy Fibers
	30		15	Fine Nanofibers
600,000	2.5	300	7.5	Beaded Fibers
	4.5		13.5	Fine Nanofibers
	5		15	Fine Nanofibers
900,000	2	450	9	Beads
	3		13.5	Film
	4		18	Fine Nanofibers
5,000,000	0.5	2500	12.5	Film
	0.6		15	Beaded Fibers
	1		25	Few Fibers + Film

Figure 4.10 (a) The relationship between the entanglement number ($(n_e)_{soln}$) and the morphology of the electrospun product

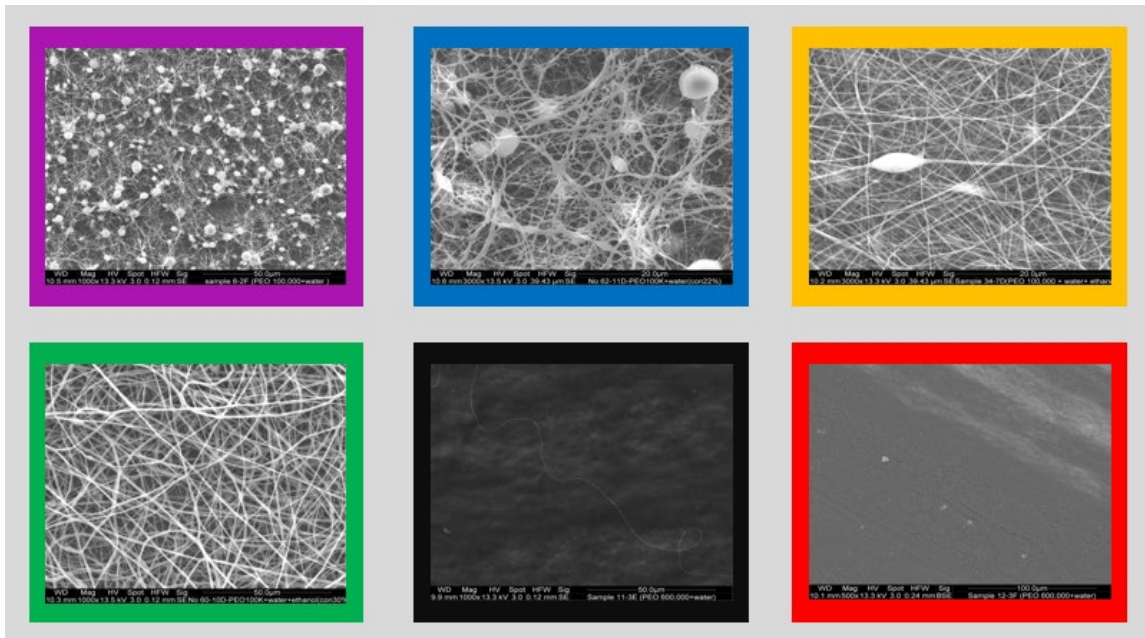


Figure 4.10 (b) SEM color-coded micrographs to correspond to a particular morphology produced by electrospinning

To further investigate the effects of molecular weight, concentration, and entanglement number on the product form, plots have been made of calculated $(n_e)_{soln}$ vs. concentration. Superimposed on these plots are an “area map” showing the regions where nanofibers, and other products, are formed. Such plots were first constructed by Shenoy et al. [30]. Two plots were constructed. Figure 4.11 is for the water solvent, and Figure 4.12 is for the water-ethanol solvent. The calculated $(n_e)_{soln}$, a semi-empirical number, is “solvent-blind”, and the present results showed that nanofibers were formed at a slightly lower $(n_e)_{soln}$ range in water-ethanol than in water.

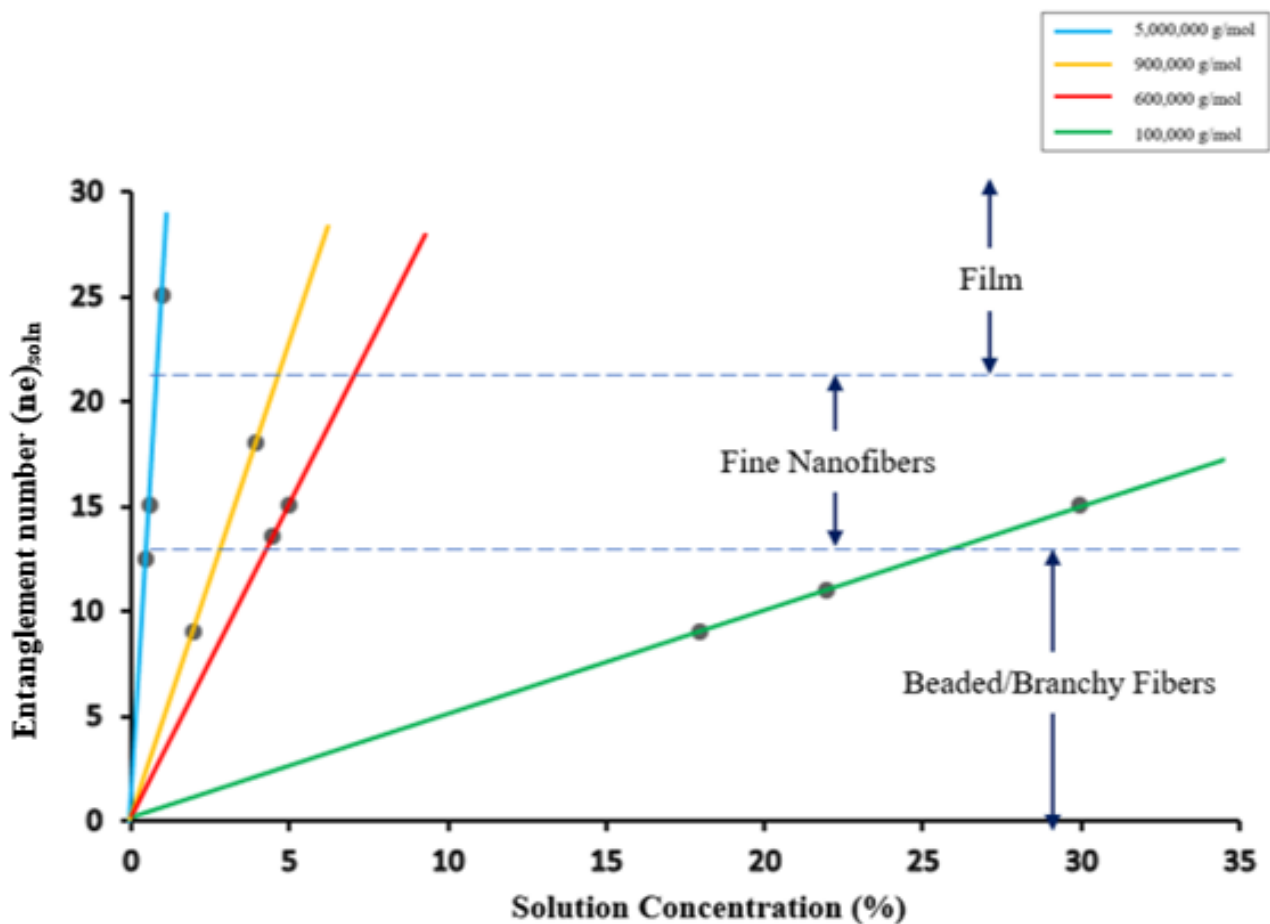


Figure 4.11 Graphic representation of solution concentration (%) vs. entanglement number (($n_e)_{soln}$) of different molecular weight of PEO in water solution

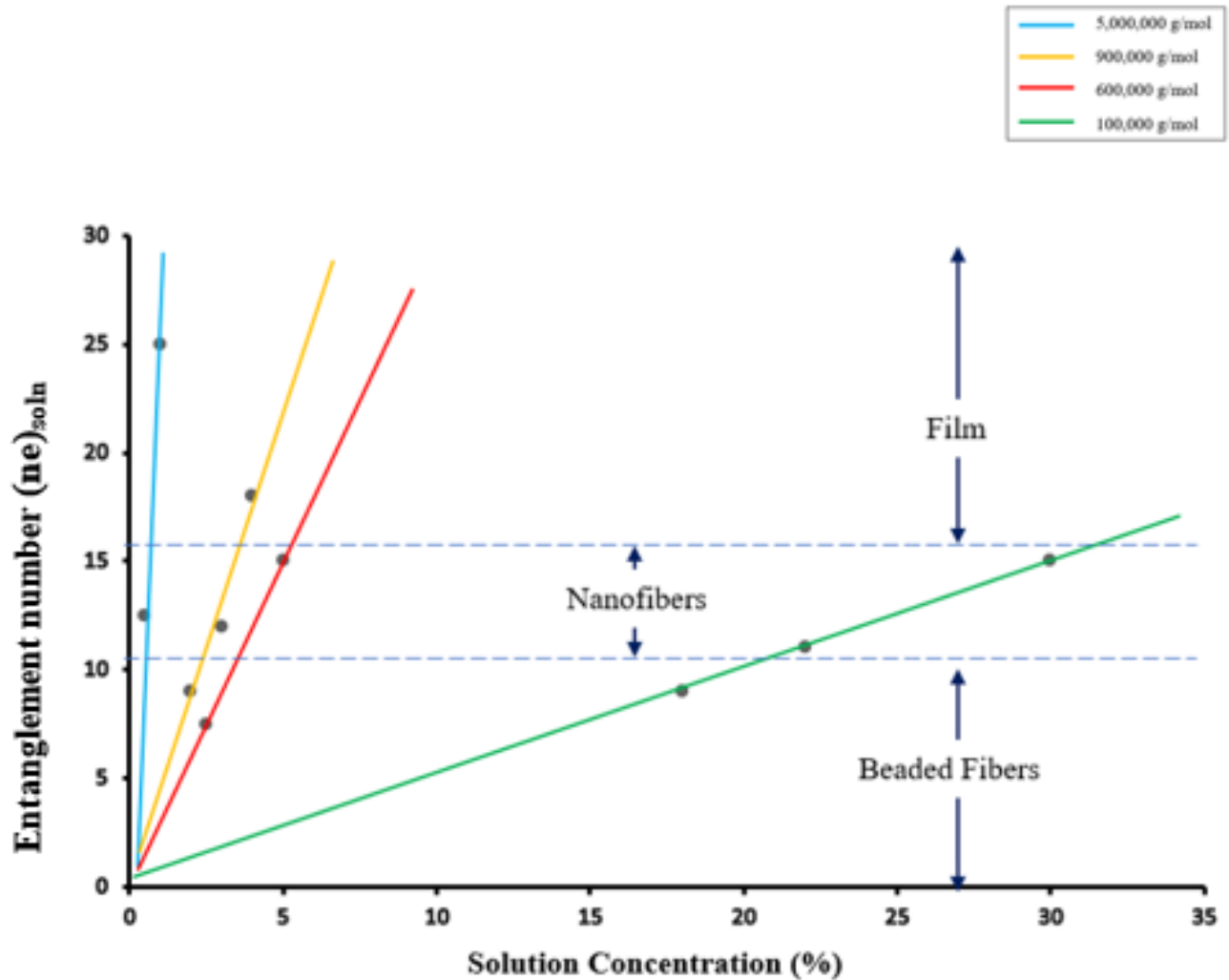


Figure 4.12 Graphic representation of solution concentration (%) vs. entanglement number ((ne)_{soln}) of different molecular weight of PEO in water-ethanol solution

4.11 References

1. Luzio, A., Canesi, E.V., Bertarelli, C., and Caironi, M. Electrospun polymer fibers for electronic applications, *Materials*, Vol. 7, pp. 906-947, (2014).
2. de Carvalho Benini, K.C.C., Cioffi, M.O.H., and Voorwald, H.J.C. PHBV/cellulose nanofibrils composites obtained by solution casting and electrospinning process, *Materia (Rio.J.)*, Vol. 22, No. 2, pp. 1-10, (2017)
3. Mark, H. in *Der feste Körper* (ed. Sanger, R.), pp. 65-104, (1938).

4. Houwink, R. Zusammenhang zwischen viscosimetrisch und osmotisch bestimmten polymerisationsgraden bei hochpolymeren. *J. Prakt. Chem*, Vol. 157, No. 15, (1940).
5. <http://www.ampolymer.com/Mark-Houwink.html>
6. Deitzel, J.M., Kleinmeyer, J., Harris, D., and Beck Tan, N.C. The effect of processing variables on the morphology of electrospun nanofibers and textiles, *Polymer*, Vol. 42, No. 1, pp. 261-272, (2001).
7. Tungprapa, S., Puangparn, T., Weerasombut, M., Jangchud, I., Fakum, P., Semongkhon, S., Meechaisue, C., and Supaphol, P. Electrospun cellulose acetate fibers: effect of solvent system on morphology and fiber diameter. *Cellulose*, Vol. 14, pp. 563–575, (2007).
8. Veleirinho, B., Rei, M.F., and Lopes-DA-Silva, J. Solvent and concentration effects on the properties of electrospun poly (ethylene terephthalate) nanofiber mats, *J. Polym. Sci., Part B: Polymer Physics*, Vol. 46, No. 5, pp. 460-471, (2008).
9. Zhang, S. Mechanical and physical properties of electrospun nanofibers, M. S. Thesis, North Carolina State University, <http://www.lib.ncsu.edu/resolver/1840.16/179>, (2009)
10. Ramakrishna, S., Fujihara, K., Teo, W.E., Lim, T.C., and Ma, Z. *An Introduction to Electrospinning and Nanofibers*, World Scientific, Singapore, 2005.
11. Mit-uppatham, C., Nithitanakul, M., and Supaphol, P. Ultrafine electrospun polyamide-6 fibers: effect of solution conditions on morphology and average fiber diameter, *Macromolecular Chemistry and Physics*, Vol. 205, No. 17, pp. 2327-2338, (2004).
12. Shamim, Z., Saeed, B., Amir, T., Abo Saied, R., and Rogheih, D. The effect of flow rate on morphology and deposition area of electrospun nylon 6 nanofiber, *J. Eng. Fabrics Fibers*, Vol. 7, No. 4, pp. 42-46, (2012).
13. Laudenslager, M.J., and Sigmund, W.M. Electrospinning, *Encyclopedia of Nanotechnology*, Springer Publishers, pp. 769–775, (2012).
14. Sill, T.J., and von Recum, H.A. Electrospinning: applications in drug delivery and tissue engineering, *Biomaterials*, Vol. 29, No. 13, pp. 1989-2006, (2008).

15. Matabola, K.P., and Moutloali, R.M. The influence of electrospinning parameters on the morphology and diameter of poly (vinylidene fluoride) nanofibers-effect of sodium chloride, *Journal of Material Science*, Vol. 48, No. 16, pp. 5475- 5482, (2013).
16. Bhardwaj, N., and Kundu, S.C. Electrospinning: a fascinating fiber fabrication technique, *Biotechnology Advances*, Vol. 28, No. 3, pp. 325-347, (2010).
17. Baumgarten, P.K. Electrostatic spinning of acrylic microfibers, *Journal of Colloid and Interface Science*, Vol. 36, No. 1, pp. 71-79, (1971).
18. Wang, T., and Kumar, S. Electrospinning of polyacrylonitrile nanofibers, *Journal of Applied Polymer Science*, Vol. 102, No. 2, pp. 1023-1029, (2006).
19. Megelski, S., Stephens, J.S., Bruce Chase, D., and Rabolt, J.F. Micro- and nanostructured surface morphology on electrospun polymer fibers, *Macromolecules*, Vol. 35, No. 22, pp. 8456-8466, (2002).
20. Zeleny, J. The role of surface instability in electrical discharges from drops of alcohol and water in air at atmospheric pressure, *Journal of Franklin Institute*, Vol. 219, No. 6, pp. 659-675, (1935).
21. Reneker, D.H., Kataphinan, W., Theron, A., Zussman, E., and Yarin, A.L. Nanofiber garlands of polycaprolactone by electrospinning, *Polymer*, Vol. 43, No. 25, pp. 6785-6794, (2002).
22. Theron, S., Zussman, E., and Yarin, A. Experimental investigation of the governing parameters in the electrospinning of polymer solutions, *Polymer*, Vol. 45, No. 6, pp. 2017-2030, (2004).
23. Harding, S.E. Intrinsic Viscosity. In: Roberts, G.C.K. (eds), *Encyclopedia of Biophysics*, Springer: Berlin/Heidelberg, (2013).
24. Kashmola, T.O., and Kamil, E.S. Structure rheology of polyethylene oxide solution, *Iraqi Journal of Chemical and Petroleum Engineering*, Vol. 15, No. 1, pp. 23-32, (2014).

25. Doshi, J., and Reneker, D.H. Electrospinning process and applications of electrospun fibers, *Journal of Electrostatics*, Vol. 35, pp. 151–160, (1995).
26. Wool, R.P. Polymer Entanglements, *Macromolecules*, Vol.26, pp 1564-1569, (1993).
27. Mckee, M.G., Wilkes, G.L., Colby, R.H., and Long, T.E. Correlation of solution rheology with electrospun fiber formation of linear and branched polymers, *Macromolecules*, Vol. 37, No. 5, pp. 1760-1767, (2004).
28. Flores-Hernandez, D.R., Cardenas-Benitez, B., Martinez-Chapa, S.O., and Bonilla-Rios, J. Tailoring the diameters of electro-mechanically spun fibers by controlling their Deborah numbers, *Polymers*, Vol. 12, Article 1358, pp 1-14, (2020).
29. Salas, B. Solution electrospinning of nanofibers. In: *Electrospun Nanofibers*, Ed. Mehdi Afshari, Cambridge, UK: Woodhead Publishing, pp. 73-108, (2016).
30. Shenoy, S.L., Bates, W.D., Frisch, H. L., Wnek, G. E. Role of chain entanglements on fiber formation during electrospinning of polymer solutions: good solvent, non-specific polymer-polymer interaction limit, *Polymer*, Vol. 46, pp. 3372-3384, (2005).
31. polymerdatabase.com/polymers/polyethyleneglycol.html
32. Fetters, L.J., Lohse, D.J., Richter, D., Witten, D., and Zirkel, A. Connection between polymer molecular weight, density, chain dimensions, and melt viscoelastic properties, *Macromolecules*, Vol. 27, No. 17, pp. 4639-4647, (1994).

CHAPTER 5

CONCLUSIONS AND SUGGESTIONS FOR FUTURE WORK

5.1 Conclusions

As noted in the Introduction, the proposed research involved two phases, namely:

1. Design and construction of purpose-built electrospinning equipment.
2. Exploratory study to examine the effect of material and processing parameters on the production of nanofibers of PEO.

The advances made and any conclusions, tentative or otherwise, are discussed separately for the two phases of the research.

5.1.1 Electrospinning equipment

The Electrospinning equipment was designed and fabricated. Full details of the equipment can be found in section 3.1 of this thesis.

Following some initial testing and modification, the equipment was successfully used for the exploratory study of the effects of material and processing parameters on the production of nanofibers of PEO.

5.1.2 Exploratory study

In the electrospinning process, a polymer solution is subjected to a high voltage electric field, in the order of tens of kV. Viscoelastic jets flow from what is called Taylor cones [1], which are formed at the polymer surface. The material of the jets, i.e., the polymer solution, after traveling a distance, typically 10-20 cm, and after evaporation of the solvent, is accumulated on an earthed collector. The electrospun product form can vary, but under specific conditions, nanofibers can be formed. For nanofiber formation, the process starts with the stable motion of the polymer solution towards a collector. This is followed by a 'whipping' motion (unstable), solvent evaporation, and finally, conversion to solid nanofibers.

The nature of the electrospun product depends on both the material parameters and the process parameters. The material parameters have also been referred to as the "entry parameters" since this is basically what is put into the electrospinning process [2].

The materials and processing parameters that were investigated in the exploratory study are summarized in Figure 5.1.

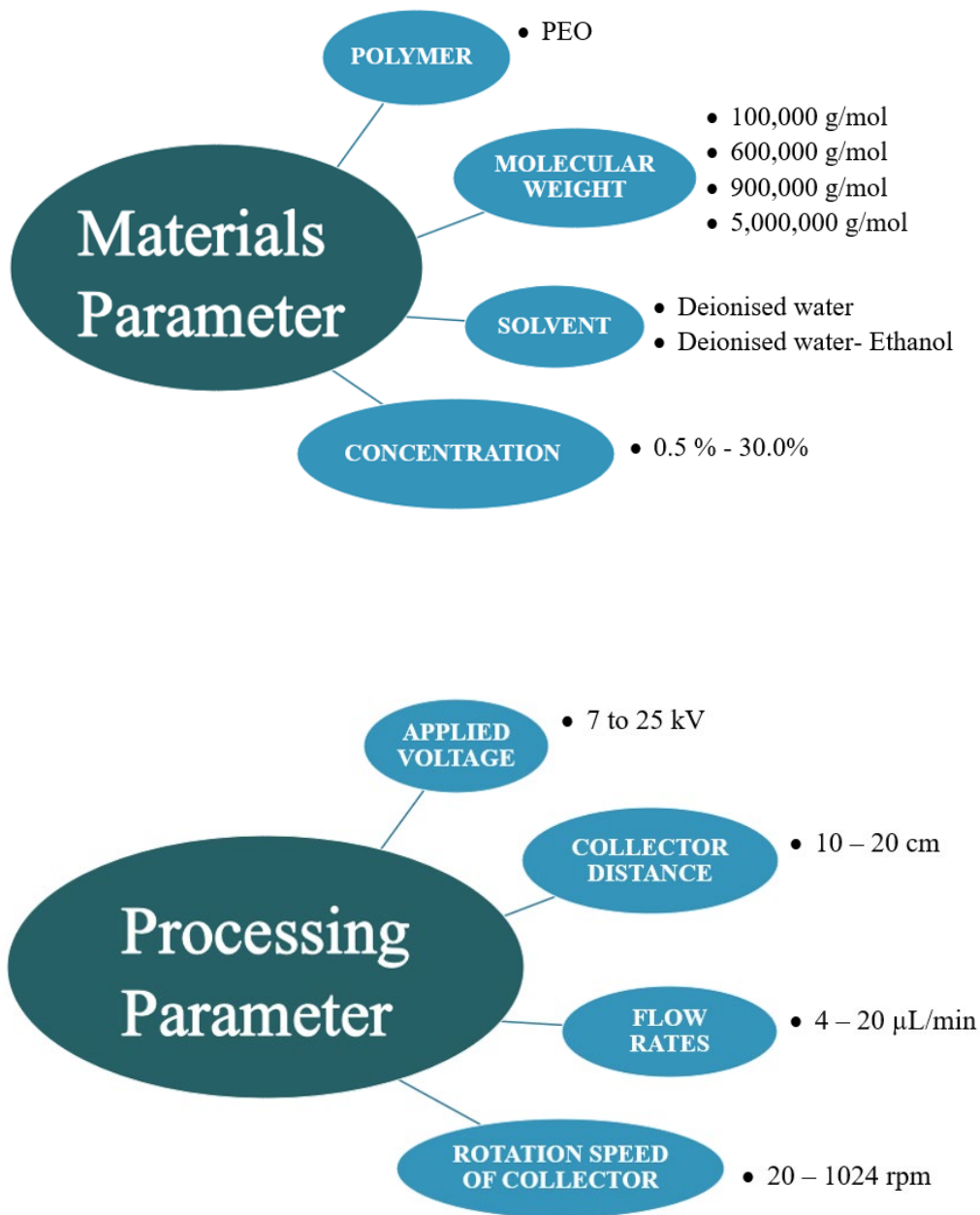


Figure 5.1 Summary of materials and processing parameters investigated in the exploratory study.

The primary focus of the study was the effect of the molecular weight of the PEO. It is readily admitted that there are quite a large number of "parameters" examined and that, as noted by Filip and Peer [2], the electrospinning process is so complex that there is no possibility to predict some characteristic of the product, in their case fiber diameter, from one of the other parameters (in our case Mw), since many parameters are interlaced.

Given these limitations, and within the confines of the parameters examined, a range of electrospun product was formed from beads (droplets) to a film deposit. Under certain material/processing conditions, nanofibers were formed.

Within the confines of the parameters examined, the materials parameters were found to have a greater effect on the product form than the processing parameters. To some extent, this is not surprising since what you put in, the "entry" parameters, will determine to a large extent what is the product. However, when the materials parameters are within the general range to produce nanofibers, changes to processing parameters such as distance from the nozzle to a collector, applied voltage, and flow rates can change the fiber morphology (smooth vs. beaded) and fiber diameter.

With respect to the effects of the materials parameters, in particular, the Mw, the importance of polydispersity was recognized. Polydispersity is where the polymer is composed of chain lengths that vary over a range of molecular masses. Thus, PEO with a nominal Mw, when dissolved in water, can have viscosities that vary over a wide range. This has implications for the electrospinning process.


The results of the exploratory study are analyzed in terms of both the viscosity and entanglement number $(n_e)_{\text{soln}}$. Nanofibers are typically formed over a viscosity range. As noted, polydispersity gives rise to variations in viscosity for the same nominal molecular weight. The entanglement number represents the physical entanglement of the PEO long linear molecular chains. The greater the concentration of PEO, the greater the number of physical entanglements. There is a $(n_e)_{\text{soln}}$ threshold that must be needed before fibers are formed. Below this threshold, beads, or beaded fibers, are formed. This threshold $(n_e)_{\text{soln}}$ would change for different solvents. The present results suggest that for PEO, this threshold $(n_e)_{\text{soln}}$ lies in the range of 13.5- 15.0. This could be most readily attained with PEO of a molecular weight of 600,000 g/mol. The use of high molecular

weight PEO (900,000 g/mol or 5,000,000 g/mol) leads to the production of a film. Also, the 5,000,000 g/mol PEO was very difficult to dissolve in water.

5.2 *Suggestions for future work*

Based on both this exploratory work and an extensive review of the literature that has come out since the present study was initiated, two future areas for research are suggested.

1. As emphasized in section 5.1, the morphology of any electrospun material depends on both the material (entry) parameters and the processing parameters. Many of these parameters are interrelated, e.g., molecular weight, concentration, and viscosity. To further investigate the effect(s) of molecular weight on the morphology of the nanofibers, a Design of Experiment (DoE) should be conducted where many of the processing parameters, such as applied voltage, needle-to-collector distance, and flow rate, be set. The effects of solution concentration and molecular weight could then be measured. Since the viscosity of the solution is one of the controlling parameters in electrospinning, the viscosity should be measured for every solution. Viscosity can also be used as a measure of the polydispersity for a given "nominal" molecular weight of the PEO.

2. In order for electrospinning to become a large-scale industrial process for the production of polymer nanofibers, better control of the process is required. As pointed out by Liu, White, and Reneker [3], on-line control requires the real-time monitoring of many electrical parameters (voltage and current) in the system: see Figure 5.2. They have proposed four locations for the monitoring of the current [3]: indicated by  in Figure 5.2. These include:
 - i. Electrical current leaving the power supply.
 - ii. Electrical current to the syringe pump.
 - iii. Electrical current from the collector.
 - iv. Current paths established by corona discharges at the surfaces of the electrospinning jets (an aluminum sheet can serve as a corona discharge detector).

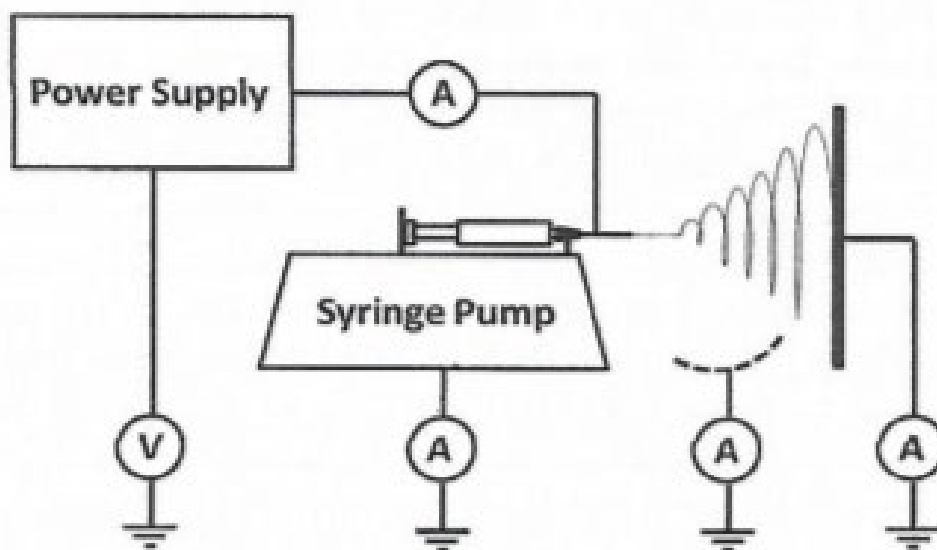


Figure 5.2 Electrospinning setup consisting of a high-voltage power supply, a syringe, a syringe pump, and a nanofiber collector (illustrated as seen from the edge of a black flat plate) [3].

The current purpose-built electrospinning equipment could be enhanced by the incorporation of instrumentation to measure these voltages and currents in a real-time manner. In the present set-up, it is impractical to measure the current to the syringe pump.

5.3 References

1. Taylor, G.I, Electrically driven jets, Proceedings of the Royal Society A, Vol. 313, pp. 453-475 (1969).
2. Filip, P., Peer, P., Characterization of poly (ethylene oxide) nanofibers – mutual relations between mean diameter of electrospun nanofibers and solution characteristics. Processes, Vol. 7, Paper 948, pp. 1-9 (2019).
3. Liu, B., White, K.L., Reneker, D.H., Electrospinning polymer nanofibers with controlled diameters, IEEE Transactions on Industry Applications, Vol.55, No. 5, pp. 5239-5243 (2019).

PRESENTATIONS, PAPERS, AND ABSTRACTS DURING M.A.Sc. STUDY

1. Northwood, D.O., Faldu, N., "Corrosion: The Circular Materials Economy and Design for Sustainability". Presented at Corrosion & Prevention 2019, Melbourne, Australia, November 24-27, 2019. Paper published in Proceedings (Australasian Corrosion Association), Paper 73, pp. 1-15 (2019).
2. Northwood, D.O., Faldu, N., Borojeni, I.A., Riahi, R., "Electrospinning of Polymeric Nanofibres : Effect of Material and Processing Parameters", Plenary Address (Abstract Only), International Conference on Nano Research and Development (ICNRD-2020), Singapore, March 12-14, 2020. *Due to COVID-19, conference is tentatively rescheduled to March 2021.

VITA AUCTORIS

NAME: Nehal Faldu

PLACE OF BIRTH: Gujarat, India

YEAR OF BIRTH: 1996

EDUCATION: B.E. Nanotechnology
Gujarat Technological University
Gujarat, India
2013-2017

M.A.Sc. Materials Engineering
University of Windsor
Windsor, Ontario
2018-2020